Summary. — In this article we will give an overview of two extensions of ground state density functional theory (DFT) – time-dependent DFT (TDDFT), and DFT for superconductors (SCDFT) – and their interplay with the electron gas. TDDFT can be viewed as an alternative formulation of time-dependent quantum mechanics that uses the electronic density as the basic variable. This theory is capable of tackling many-electron systems under the influence of a generic time-dependent external potential (such as a laser field). Furthermore, TDDFT is a very powerful tool to calculate linear excitation spectra. On the other hand, SCDFT is an attempt to describe the phenomenon of superconductivity from a density functional perspective. In all these density functional theories, the complexities of the many-body problem are included in the so-called exchange-correlation functional. This is a very complicated quantity that has to be approximated in any practical application of the theory. One of the most successful approximate exchange-correlation functionals is certainly the local density approximation, which uses information from the uniform electron gas to construct an exchange-correlation functional for the inhomogeneous system. Local density approximations have been proposed both within TDDFT and SCDFT. We will pay particular attention to their construction and, whenever possible, give a critical account of their successes and failures.

The electron gas in TDDFT and SCDFT

MIGUEL A. L. MARQUES and EBERHARD K. U. GROSS

Institut für Theoretische Physik, Freie Universität Berlin, Arnimallee 14, D-14195 Berlin, Germany

1. – Introduction

1˙1. *The electron gas paradigm.* – As most physicists, the reader probably owns at least a shelf-full of physics books, some technical and specialized, others remnant from undergraduate studies, some acquired to satisfy the insatiable curiosity that characterizes scientists. Among these books, one will very likely find a couple about many-body physics, and several that treat the subject of solid state physics or condensed matter theory. By opening any of these books, the reader will invariably encounter the electron gas. Theoretically, the electron gas is a model for a system of electrons and nuclei, where the point nuclei have been replaced by a uniform distribution of positive charge. The model thus defined exhibits translational symmetry and can be characterized, in the simplest case, by a single number, the (constant) electronic density. The complete neglect of the nuclei may seem at first as a very drastic approximation. However, this "trivial" model is still able to exhibit a wealth of different physical phenomena. At very low densities and very low temperature, several phases are in competitions: The Wigner crystal[1]; a superconducting phase first predicted by Kohn and Luttinger[2]; as well as ferromagnetic and anti-ferromagnetic phases[3]. Is is therefore not surprising that the electron gas is used as an almost ubiquitous paradigm in solid state physics.

Traditionally, simple models (like the electron gas) are used to understand the physics of complicated systems. Stripped out of successive layers of unnecessary detail, the model pinpoints the basic underlying causes, and explains qualitatively the behavior of the system. Some useful information can normally be extracted, like asymptotic behaviors, scaling properties, etc. What is usually beyond the reach of a simple model is the calculation of specific properties of specific systems. But the electron gas surprises us once again – when information obtained from the gas is used in the context of density functional theory (DFT)[4, 5, 6], one obtains one of the most reliable methods to calculate ground-state properties of real materials.

In this article we will be concerned with two extensions of the traditional ground-state DFT – time-dependent DFT (TDDFT), and DFT for superconductors (SCDFT) – and with their interplay with the electron gas. TDDFT was proposed by Runge and Gross in 1984 as a tool to study electronic systems under the influence of an external time-dependent field (such as an electromagnetic field)[7]. More recently it has become very popular for the calculation of linear excitation spectra, and is by now deployed in most quantum-chemistry codes. The less known SCDFT is an attempt to tackle the problem of superconductivity from the density functional perspective[8, 9]. The evolution of SCDFT has been slow, but recent developments may pave the way for a more general use of this theory[10, 11, 12].

However, before entering the realm of TDDFT and SCDFT, we will give a brief

overview of the basic ideas of ground-state DFT, that will allow us to fix some basic notation that will be used in the rest of this article, and to introduce some key concepts that will be developed later. Hartree atomic units will be used throughout this article, unless explicitly stated.

1˙2. *Ground-state density functional theory.* – The basic quantity in quantum mechanics is the wave-function. From the wave-function all observables of the system can be easily obtained just by taking the expectation value of the appropriate operator. Unfortunately, the wave-function is a rather "clumsy" quantity to work with – For a system of N electrons, the many-body wave-function is a complex function of $3N$ variables (the three coordinates of each electron, and ignoring the spin degrees of freedom). For a simple nitrogen atom (7 electrons) this amounts to 21 coordinates. Clearly, a function of 21 coordinates can *not* be evaluated or even stored in a modern computer. Fortunately, an electronic quantum system can be fully described by simpler functions, like the two-particle density matrix[13], the one-particle density matrix[14], or even by the much simpler electronic density[15]. In the following we will be concerned with this latter function, the density, which plays the central role in DFT. The density can be written as the expectation value of the operator

$$\hat{n}(\boldsymbol{r}) = \sum_{\sigma} \hat{n}_{\sigma}(\boldsymbol{r}) \quad ; \quad \hat{n}_{\sigma}(\boldsymbol{r}) = \hat{\psi}^{\dagger}_{\sigma}(\boldsymbol{r})\hat{\psi}_{\sigma}(\boldsymbol{r})\,, \tag{1}$$

where $\hat{\psi}_{\sigma}(\boldsymbol{r})$ [$\hat{\psi}^{\dagger}_{\sigma}(\boldsymbol{r})$] annihilates [creates] a particle of spin σ at position $\boldsymbol{r}$. With the help of the Rayleigh-Ritz principle it is possible to prove the following three statements, that constitute the celebrated Hohenberg-Kohn theorem[15]

1. The electronic density of an interacting system of electrons fully and uniquely determines the external potential, $v(\boldsymbol{r})$, that these electrons experience and thus the Hamiltonian, the many-body wave-function, and all observables of the system.
2. The ground-state energy of this system can be obtained by minimizing the total energy in terms of the density.
3. There exists a functional $F[n]$([1]) such that the total energy, $E[n]$, can be written in the form

$$E[n] = F[n] + \int \mathrm{d}^3 r\, n(\boldsymbol{r}) v(\boldsymbol{r})\,. \tag{2}$$

The functional F is universal, in the sense that its functional dependence on the density is the same for all systems with the same particle-particle interaction.

While, in principle, one could work with the density alone, in practise it is favorable to employ an explicitly spin-dependent version of DFT[16] where the total energy E and

([1]) By $[n]$ we denote a functional dependence on n.

the universal functional F are explicit functionals of the spin-densities $n_\downarrow$, $n_\uparrow$. In the following we will deal exclusively with spin-DFT.

The Hohenberg-Kohn theorem is an existence theorem – it proves that the ground-state of the system can be obtained from the density alone, but, unfortunately, it does not teach us how to do it in practice. A practical framework was developed by Kohn and Sham in 1965[17]. Their idea was to construct a simple auxiliary system of non-interacting electrons with the same density as the interacting system. As the Kohn-Sham system is non-interacting, its ground-state can be obtained by solving the one-particle Schrödinger equation

$$\left[-\frac{\nabla^2}{2} + v_\sigma^{\mathrm{KS}}[n_\uparrow, n_\downarrow](\boldsymbol{r})\right] \varphi_{i\sigma}(\boldsymbol{r}) = \epsilon_{i\sigma}\varphi_{i\sigma}(\boldsymbol{r})\,. \tag{3}$$

The ground-state spin-densities can then be calculated as a sum over the N_σ lowest occupied Kohn-Sham states

$$n_\sigma(\boldsymbol{r}) = \sum_i^{N_\sigma} |\varphi_{i\sigma}(\boldsymbol{r})|^2\ , \tag{4}$$

where N_σ is the number of electrons with spin σ. The external potential that the Kohn-Sham electrons feel is usually separated into three parts

$$v_\sigma^{\mathrm{KS}}[n_\uparrow, n_\downarrow](\boldsymbol{r}) = v_\sigma(\boldsymbol{r}) + \int \mathrm{d}^3r'\, \frac{n(\boldsymbol{r}')}{|\boldsymbol{r}-\boldsymbol{r}'|} + v_\sigma^{\mathrm{xc}}[n_\uparrow, n_\downarrow](\boldsymbol{r})\,. \tag{5}$$

The first, $v_\sigma(\boldsymbol{r})$, is the external potential (usually created by a set of nuclear charges). Then comes the Hartree potential, which accounts for the classical part of the interaction between the electrons. Finally, we have the exchange-correlation (xc) potential, $v_\sigma^{\mathrm{xc}}[n_\uparrow, n_\downarrow](\boldsymbol{r})$, that includes all non-trivial many-body effects. This term can be written as the functional derivative of the xc energy

$$v_\sigma^{\mathrm{xc}}[n_\uparrow, n_\downarrow](\boldsymbol{r}) = \frac{\delta E_{\mathrm{xc}}[n_\uparrow, n_\downarrow]}{\delta n_\sigma(\boldsymbol{r})}\,. \tag{6}$$

Finally, the xc energy can be defined with the help of the functional $F[n_\uparrow, n_\downarrow]$ by the equation

$$F[n_\uparrow, n_\downarrow] = T_{\mathrm{s}}[n_\uparrow, n_\downarrow] + E_{\mathrm{Hartree}} + E_{\mathrm{xc}}[n_\uparrow, n_\downarrow]\,, \tag{7}$$

where $T_{\mathrm{s}}[n_\uparrow, n_\downarrow]$ is the kinetic energy of the system of non-interacting electrons, and the Hartree energy has the definition

$$E_{\mathrm{Hartree}} = \frac{1}{2}\int \mathrm{d}^3r \int \mathrm{d}^3r'\, \frac{n(\boldsymbol{r})n(\boldsymbol{r}')}{|\boldsymbol{r}-\boldsymbol{r}'|}\,. \tag{8}$$

If we possessed the exact xc energy functional, the Kohn-Sham equations would yield the exact density of the interacting many-body system. Unfortunately, $E_{\rm xc}$ is a very complicated quantity that has to be approximated in any practical application of the Kohn-Sham scheme. In the following we will give a brief overview of the different approximations to $E_{\rm xc}$ that are currently available, and their connection to the electron gas, the central topic of this volume.

1˙3. *Ground-state exchange-correlation functionals.* – The first approximation to the xc energy functional, the so-called local density approximation (LDA), was proposed by Kohn and Sham in 1965[17]

$$E_{\rm xc}^{\rm LDA} = \int {\rm d}^3 r \, n(\boldsymbol{r}) \varepsilon_{\rm xc}^{\rm unif}(n_\uparrow(\boldsymbol{r}), n_\downarrow(\boldsymbol{r}))\,, \tag{9}$$

where $\varepsilon_{\rm xc}^{\rm unif}(n_\uparrow, n_\downarrow)$ is the energy per particle of the homogeneous electron gas with (constant) spin-densities $n_\uparrow$ and $n_\downarrow$ – a quantity well known from, e.g., quantum Monte-Carlo calculations[18]. The LDA functional is *local*, i.e., the energy density at the point $\boldsymbol{r}$ only depends on the density at that same point. By construction, one would expect the LDA to perform well only for systems with slowly varying densities, but, in fact, the LDA yields remarkably good results even for highly inhomogeneous systems, like atoms or small molecules.

Next in the ladder of ever increasing complexity come the generalized gradient approximations (GGAs)[19]. The general form of a GGA is

$$E_{\rm xc}^{\rm GGA} = \int {\rm d}^3 r \, f(n_\uparrow(\boldsymbol{r}), n_\downarrow(\boldsymbol{r}), \nabla n_\uparrow(\boldsymbol{r}), \nabla n_\downarrow(\boldsymbol{r}))\,. \tag{10}$$

Note that besides the local dependence on the density, the function f also depends on the gradient of the density. For this reason, the GGA is sometimes referred to as a semi-local approximation. In contrast to the LDA where $\varepsilon_{\rm xc}^{\rm unif}(n)$ is unique and known to very good accuracy, the function f in the GGA is uniquely defined only in the limit of a weakly inhomogeneous gas, i.e. in the limit where the dimensionless density gradient $\nabla n_\sigma / n_\sigma^{4/3}$ approaches zero. In this limit, f can be expressed in terms of the response functions of the uniform electron gas[15]. Beyond this limit, the common approach to obtain this function proceeds as follows: i) The function f is parameterized in some smart way. Sometimes the parameterization is crafted to give the exact xc energy for some well studied system, like the uniform electron gas. ii) Sum rules, and some other features of the exact xc functional are used to determine the unknown parameters. iii) If some parameters are still left unknown, fit them to some small molecules or other physical systems.

More recently, a new class of functionals has been proposed – the meta-GGAs[20]. Besides the usual dependence on the density and on its gradient, the meta-GGAs require

a third variable, the kinetic energy density

$$\tau_\sigma(\boldsymbol{r}) = \frac{1}{2}\sum_i^{\text{occ}} |\nabla\varphi_{i\sigma}(\boldsymbol{r})|^2 \,. \tag{11}$$

The energy functional then takes the form

$$E_{\text{xc}}^{\text{MGGA}} = \int \mathrm{d}^3r\, g(n_\uparrow(\boldsymbol{r}), n_\downarrow(\boldsymbol{r}), \nabla n_\uparrow(\boldsymbol{r}), \nabla n_\downarrow(\boldsymbol{r}), \tau_\uparrow(\boldsymbol{r}), \tau_\downarrow(\boldsymbol{r}))\,. \tag{12}$$

The function g is determined in the same way as in the GGA. The extra flexibility gained by the introduction of τ allowed to improve the results obtained with the traditional GGAs. Note that $E_{\text{xc}}^{\text{MGGA}}$ is no longer an *explicit* density functional, but depends on the Kohn-Sham orbitals due to the τ dependence. The orbitals are solutions of the Kohn-Sham equation, and therefore functionals of the Kohn-Sham potential. This latter quantity is, by virtue of the Hohenberg-Kohn theorem, a functional of the density which proves that $E_{\text{xc}}^{\text{MGGA}}$ is still a density functional, although its functional dependence on the density is *implicit*.

Another orbital functional (or implicit density functional) that we will encounter in the following is the exact exchange (EXX)[21, 22]. It stems from a perturbative expansion in e^2 of the xc energy (where e is the electron charge), and reads

$$E_{\text{x}}^{\text{EXX}} = -\frac{1}{2}\sum_\sigma \sum_{i,j}^{\text{occ}} \int \mathrm{d}^3r \int \mathrm{d}^3r'\, \frac{\varphi_{i\sigma}(\boldsymbol{r})\varphi^*_{i\sigma}(\boldsymbol{r}')\varphi_{j\sigma}(\boldsymbol{r}')\varphi^*_{j\sigma}(\boldsymbol{r})}{|\boldsymbol{r}-\boldsymbol{r}'|}\,. \tag{13}$$

This functional has exactly the same form as the Fock term in Hartree-Fock theory. However, the functional (13) should be evaluated with the Kohn-Sham orbitals – which are solutions of a Schrödinger equation with a local potential – and not with the Hartree-Fock orbitals – that stem from a free minimization of the energy in terms of the orbitals. This subtle difference has some quite profound consequences for some systems – e.g, the electron gas calculated with the EXX functional does not exhibit the pathologies at the Fermi surface present in the Hartree-Fock solution.

A very important problem that affects the LDA (and most GGAs and meta-GGAs) is the presence of a spurious self-interaction term. This problem can be easily understood by writing the Hartree energy in terms of the orbitals

$$E_{\text{Hartree}} = \frac{1}{2}\sum_{\substack{ij\\ \sigma\sigma'}} \int \mathrm{d}^3r \int \mathrm{d}^3r'\, \frac{|\varphi_{i\sigma}(\boldsymbol{r})|^2|\varphi_{j\sigma'}(\boldsymbol{r}')|^2}{|\boldsymbol{r}-\boldsymbol{r}'|}\,. \tag{14}$$

Note that the $i = j$, $\sigma = \sigma'$ term is included in the sum. This term, usually called the self-interaction part of the Hartree energy, has a simple interpretation: It describes the interaction of an electron with itself. It is clearly a spurious term, that should be canceled by a similar diagonal term coming from the exchange contribution to the energy

[cf. eq. (13)]. However, most approximations to the exchange energy functional – like the LDA or the GGA – do *not* cancel the self-interaction part of the Hartree energy, which leads to some well known pathologies. For example, the exact xc potential for a neutral finite system decays asymptotically as $-1/r$, while the LDA potential goes exponentially to zero. The LDA potential is consequently too shallow, the Kohn-Sham eigenvalues are too small, and the system has problems binding extra electrons. This problem is particularly severe when performing time-dependent calculations within the LDA, for the ionization probability is greatly overestimated.

Approximate correlation functionals may also include spurious self-interaction terms. It is clear that for a one-particle system the correlation energy has to vanish. While this is true for the more recent meta-GGAs[20], the LDA and GGA correlation functionals are *not* zero for one-particle systems.

In 1981, Perdew and Zunger had the idea of subtracting all these spurious self-interaction terms from the LDA energy functional[23]. The resulting SIC functional reads

(15)
$$E_{\rm xc}^{\rm SIC} = E_{\rm xc}^{\rm LDA}\left[n_\uparrow, n_\downarrow\right] - \sum_{i\sigma} E_{\rm xc}^{\rm LDA}\left[\left|\varphi_{i\sigma}\right|^2, 0\right] - \frac{1}{2}\sum_{i\sigma}\int {\rm d}^3r \int {\rm d}^3r' \, \frac{\left|\varphi_{i\sigma}(\boldsymbol{r})\right|^2 \left|\varphi_{i\sigma}(\boldsymbol{r}')\right|^2}{|\boldsymbol{r}-\boldsymbol{r}'|}.$$

The SIC is, by construction, fully self-interaction free, so the SIC potential has the correct $-1/r$ asymptotic behavior for neutral finite systems. However, this functional suffers from a different pathology: expression (15) is not invariant upon unitary transformations of the Kohn-Sham orbitals.

The success of DFT is based on the availability of increasingly accurate approximations to the xc energy functional. Currently, the most promising line of research are orbital functionals, but the quest for still more accurate approximations continues.

2. – Time-dependent density functional theory

Ordinary DFT is concerned with systems subject to a static external potential, which are described by the *time-independent* Schrödinger equation. However, there are many situations of interest that fall outside this category. A few examples are: an atom or a molecule under the influence of an external electromagnetic field (like a laser field), electron or proton scattering, etc. These systems are correctly described by the *time-dependent* Schrödinger equation. TDDFT is an extension of ordinary ground-state DFT designed to tackle such problems from a density functional perspective.

The theoretical foundations of TDDFT were laid down by Runge and Gross in 1984[7], who proved a Hohenberg-Kohn like theorem and developed a Kohn-Sham scheme for the time-dependent case. Although their original motivation was the description of scattering experiments, the formalism is general enough to encompass other time-dependent problems. In fact, nowadays the most important application of TDDFT is the calculation of optical absorption spectra of finite systems.

2˙1. *Preliminaries.* – A system of N electrons subject to an arbitrary time-dependent potential obeys the time-dependent many-body Schrödinger equation

$$\mathrm{i}\frac{\partial}{\partial t}\Psi_{\underline{\sigma}}(\underline{\boldsymbol{r}},t) = \hat{H}(\underline{\boldsymbol{r}},t)\Psi_{\underline{\sigma}}(\underline{\boldsymbol{r}},t)\,, \tag{16}$$

where $\hat{H}$ is the Hamilton operator of the system, $\underline{\sigma} = (\sigma_1 \cdots \sigma_N)$ are the spin coordinates, and $\underline{\boldsymbol{r}} = (\boldsymbol{r}_1 \cdots \boldsymbol{r}_N)$ are the spatial coordinates of the N electrons. The Hamiltonian is naturally decomposed into three terms

$$\hat{H}(\underline{\boldsymbol{r}},t) = \hat{T}(\underline{\boldsymbol{r}}) + \hat{U}(\underline{\boldsymbol{r}}) + \hat{V}(\underline{\boldsymbol{r}},t)\,. \tag{17}$$

The first term accounts for the kinetic energy of the electrons, while the second is the electron-electron interaction

$$\hat{T}(\underline{\boldsymbol{r}}) = -\sum_i \frac{\nabla_i^2}{2} \quad ; \quad \hat{U}(\underline{\boldsymbol{r}}) = \frac{1}{2}\sum_{i\neq j}\frac{1}{|\boldsymbol{r}_i - \boldsymbol{r}_j|}\,, \tag{18}$$

where the $1/2$ in the definition of $\hat{U}$ was introduced to avoid double counting. The electrons evolve under the influence of the external time-dependent potential $\hat{V}$. In this article we will only be concerned with external potentials that can be written as a sum of one-body terms

$$\hat{V}(\underline{\boldsymbol{r}},t) = \sum_i v(\boldsymbol{r}_i,t)\,. \tag{19}$$

Most potentials that appear in condensed-matter physics are of this kind. For example, a system of N_n nuclei (treated as *classical* particles moving on trajectories $\boldsymbol{R}_\nu(t)$) will produce the potential

$$v(\boldsymbol{r},t) = -\sum_{\nu=1}^{N_\mathrm{n}}\frac{Z_\nu}{|\boldsymbol{r} - \boldsymbol{R}_\nu(t)|}\,, \tag{20}$$

where Z_ν denotes the charge of the nucleus ν.

Also electromagnetic fields can be easily described by (19). For example, if we shine a laser beam on an electronic system, the electrons will feel the potential (in the dipole approximation)

$$v(\boldsymbol{r},t) = E\, f(t)\, \sin(\omega t)\boldsymbol{r}\cdot\boldsymbol{\alpha}\,, \tag{21}$$

where $\boldsymbol{\alpha}$, ω and E are the polarization, the frequency and the amplitude of the laser, respectively. The function $f(t)$ is an envelope that describes the temporal shape of the laser pulse. The dipole approximation is a commonly used approximation that holds whenever the following conditions are true: i) The wave-length of the light ($\lambda = 2\pi c/\omega$,

where c is the velocity of light in vacuum) is much larger than the size of the system. ii) The path that the particle travels in one period of the laser field is small compared to the wave-length. If v is the average velocity of the electrons then $vT \ll \lambda \Rightarrow v \ll \lambda/T = c$, where T stands for the period of the laser. In these circumstances we can treat the laser field as a purely electric field and completely neglect its magnetic component. iii) The total duration of the laser pulse should be short enough so that the molecule does not leave the focus of the laser during the time the interaction lasts.

The electronic density is obtained by contracting the absolute square of the time-dependent many-body wave-function

$$n(\boldsymbol{r},t) = N \sum_{\sigma_1 \cdots \sigma_N} \int \mathrm{d}^3\boldsymbol{r}_2 \cdots \mathrm{d}^3\boldsymbol{r}_N \, |\Psi(\boldsymbol{r}\sigma_1, \boldsymbol{r}_2\sigma_2, \cdots, \boldsymbol{r}_N\sigma_N, t)|^2 \; . \tag{22}$$

With this definition, the total density n is normalized at all times to the total number of electrons, N. Another observable that we will encounter is the current density, $\boldsymbol{j}$. It has the definition

$$\begin{aligned} \boldsymbol{j}(\boldsymbol{r},t) = \frac{N}{2\mathrm{i}} \sum_{\sigma_1 \cdots \sigma_N} \int & \mathrm{d}^3\boldsymbol{r}_2 \cdots \mathrm{d}^3\boldsymbol{r}_N \\ & [\Psi^*(\boldsymbol{r}\sigma_1, \boldsymbol{r}_2\sigma_2, \cdots, \boldsymbol{r}_N\sigma_N, t) \nabla \Psi(\boldsymbol{r}\sigma_1, \boldsymbol{r}_2\sigma_2, \cdots, \boldsymbol{r}_N\sigma_N, t) - \text{c.c.}] \; . \end{aligned} \tag{23}$$

2˙2. *Basic theorems.* – The formal foundations of TDDFT are enclosed in the so-called Runge-Gross theorem[7] – the time-dependent generalization of the Hohenberg-Kohn theorem[15] – while the practical framework of the theory is given by the time-dependent Kohn-Sham scheme. One usually derives the Kohn-Sham scheme using a variational principle based on the quantum mechanical action. This has, however, to be done with care due to problems related to causality.

2˙2.1. The Runge-Gross theorem. The Runge-Gross theorem states that there exists a one-to-one correspondence between the external potential, $v(\boldsymbol{r},t)$, and the electron density, $n(\boldsymbol{r},t)$ for time-dependent systems evolving from a fixed many-body state[7]. The consequences of this statement are quite profound: Let us assume that we possess the density of an electronic system. The Runge-Gross theorem assures that this information is in principle sufficient to obtain the external potential of the system. Now, we can insert the external potential in the time-dependent Schrödinger equation and solve it, thereby obtaining the time-dependent many-body wave-function. As this wave-function determines all observables of the system, we conclude that *all observables are functionals of the time-dependent density.*

Note that the Runge-Gross theorem only holds for a *fixed* initial state, i.e., the density functionals will depend parametrically on the initial many-body state. This problem is absent, however, if the system departs, at $t = t_0$, from its ground state. By virtue of the Hohenberg-Kohn theorem, the ground state many-body wave-function is a functional of the ground state density, i.e., $n(\boldsymbol{r}, t = t_0)$. Special care has nevertheless to be taken if,

on the other hand, the system at $t = t_0$ is in an arbitrary many-body state (which is the case, e.g., in electron scattering) [24, 25].

In order to prove the Runge-Gross theorem, we assume that we have two systems with different time-dependent potentials, v and v'([2]) differing by more than a purely time-dependent constant. If the two potentials differ solely by a time-dependent function, they will produce wave-functions which are equal up to a purely time-dependent phase. This phase will, of course, cancel while calculating the density (or any other observable, in fact). Both systems evolve from the same many-body state, so, at $t = t_0$ we have

$$|\Psi(t_0)\rangle = |\Psi'(t_0)\rangle \equiv |\Psi_0\rangle \,, \tag{24a}$$

$$n(\boldsymbol{r}, t_0) = n'(\boldsymbol{r}, t_0) \equiv n^0(\boldsymbol{r}) \,, \tag{24b}$$

$$\boldsymbol{j}(\boldsymbol{r}, t_0) = \boldsymbol{j}'(\boldsymbol{r}, t_0) \equiv \boldsymbol{j}^0(\boldsymbol{r}) \,. \tag{24c}$$

In a first step one proves, using the equation of motion for the current density, that two external potentials v and v' yield different current densities $\boldsymbol{j}$ and $\boldsymbol{j}'$. In a second step, the continuity equation is used to show that if two systems have different current densities, then they must also possess different time-dependent densities, i.e., $\boldsymbol{j} \neq \boldsymbol{j}' \Rightarrow n \neq n'$. Combining these two statements we get

$$v(\boldsymbol{r}, t) \neq v'(\boldsymbol{r}, t) + c(t) \Rightarrow n(\boldsymbol{r}, t) \neq n'(\boldsymbol{r}, t) \,. \tag{25}$$

In the following we will give a detailed account of the proof of this important theorem. For reasons that will become apparent during the course of the demonstration, we require that the external potential can be expanded for $t > t_0$ in a Taylor series around the initial time t_0

$$v(\boldsymbol{r}, t) = \sum_{k=0}^{\infty} c_k(\boldsymbol{r})(t - t_0)^k \,, \tag{26}$$

with the expansion coefficients

$$c_k(\boldsymbol{r}) = \frac{1}{k!} \frac{\partial^k}{\partial t^k} v(\boldsymbol{r}, t) \bigg|_{t=t_0} \,. \tag{27}$$

This requirement is certainly fulfilled by any real-world time-dependent potential. It nevertheless excludes some cases like adiabatically switched-on potentials. Furthermore, we define the function

$$u_k(\boldsymbol{r}) = \frac{\partial^k}{\partial t^k} \left[v(\boldsymbol{r}, t) - v'(\boldsymbol{r}, t) \right] \bigg|_{t=t_0} \,. \tag{28}$$

([2]) In the following we will use primes to distinguish the quantities of the systems with external potentials v and v'.

It is clear that if $v(\boldsymbol{r},t) \neq v'(\boldsymbol{r},t) + c(t)$, then at least one of the expansion coefficients in their Taylor expansion around t_0 will differ by more than a constant

$$\exists_{k\geq 0} : u_k(\boldsymbol{r}) \neq \text{constant}. \tag{29}$$

The quantum-mechanical equation of motion, which is valid for any operator, $\hat{O}(t)$, reads

$$\mathrm{i}\frac{\mathrm{d}}{\mathrm{d}t}\left\langle\Psi(t)\right|\hat{O}(t)\left|\Psi(t)\right\rangle = \left\langle\Psi(t)\right|\mathrm{i}\frac{\partial}{\partial t}\hat{O}(t) + \left[\hat{O}(t),\hat{H}(t)\right]\left|\Psi(t)\right\rangle\,. \tag{30}$$

We will be interested in the equation of motion for the current density

$$\hat{\boldsymbol{j}}(\boldsymbol{r}) = \frac{1}{2\mathrm{i}}\sum_{\sigma}\{\hat{\psi}^{\dagger}_{\sigma}(\boldsymbol{r})\left[\nabla\hat{\psi}_{\sigma}(\boldsymbol{r})\right] - \left[\nabla\hat{\psi}^{\dagger}_{\sigma}(\boldsymbol{r})\right]\hat{\psi}_{\sigma}(\boldsymbol{r})\}\,. \tag{31}$$

Subtracting the equations of motion for the current density in the prime and unprimed systems we obtain, at $t = t_0$,

$$\begin{aligned}\mathrm{i}\frac{\partial}{\partial t}\left[\boldsymbol{j}(\boldsymbol{r},t) - \boldsymbol{j}'(\boldsymbol{r},t)\right]_{t=t_0} &= \left\langle\Psi_0\right|\left[\hat{\boldsymbol{j}}(\boldsymbol{r}),\hat{H}(t_0) - \hat{H}'(t_0)\right]\left|\Psi_0\right\rangle \\ &= \left\langle\Psi_0\right|\left[\hat{\boldsymbol{j}}(\boldsymbol{r}),v(\boldsymbol{r},t_0) - v'(\boldsymbol{r},t_0)\right]\left|\Psi_0\right\rangle \\ &= \mathrm{i}n^0(\boldsymbol{r})\nabla\left[v(\boldsymbol{r},t_0) - v'(\boldsymbol{r},t_0)\right]\,. \end{aligned} \tag{32}$$

If the two potentials, v and v', differ at t_0 [i.e., if (29) is fulfilled already with $k = 0$], the derivative on the left-hand side of (32) is different from zero, and the two current densities $\boldsymbol{j}$ and $\boldsymbol{j}'$ deviate for $t > t_0$. On the other hand, if u_k is not a constant only for $k > 0$, we can apply the equation of motion $k + 1$ times, yielding

$$\frac{\partial^{k+1}}{\partial t^{k+1}}\left[\boldsymbol{j}(\boldsymbol{r},t) - \boldsymbol{j}'(\boldsymbol{r},t)\right]_{t=t_0} = n^0(\boldsymbol{r})\nabla u_k(\boldsymbol{r})\,. \tag{33}$$

The right-hand side of (33) differs from zero, which again implies that $\boldsymbol{j}(\boldsymbol{r},t) \neq \boldsymbol{j}'(\boldsymbol{r},t)$ for $t > t_0$. This concludes the first step of the proof of the Runge-Gross theorem.

The second step of the proof, i.e., that $\boldsymbol{j} \neq \boldsymbol{j}' \Rightarrow n \neq n'$, makes use of the continuity equation

$$\frac{\partial}{\partial t}n(\boldsymbol{r},t) = -\nabla\cdot\boldsymbol{j}(\boldsymbol{r},t)\,. \tag{34}$$

Writing (34) for the primed and unprimed system and taking the difference, we arrive at

$$\frac{\partial}{\partial t}\left[n(\boldsymbol{r},t) - n'(\boldsymbol{r},t)\right] = -\nabla\cdot\left[\boldsymbol{j}(\boldsymbol{r},t) - \boldsymbol{j}'(\boldsymbol{r},t)\right]\,. \tag{35}$$

As before, we would like an expression involving the kth time derivative of the external potential, so we take the $(k+1)$st time-derivative of (35) to obtain (at $t = t_0$)

$$\begin{aligned} \frac{\partial^{k+2}}{\partial t^{k+2}} \left[n(\boldsymbol{r},t) - n'(\boldsymbol{r},t) \right]_{t=t_0} &= -\nabla \cdot \frac{\partial^{k+1}}{\partial t^{k+1}} \left[\boldsymbol{j}(\boldsymbol{r},t) - \boldsymbol{j}'(\boldsymbol{r},t) \right]_{t=t_0} \\ &= -\nabla \cdot \left[n^0(\boldsymbol{r}) \nabla u_k(\boldsymbol{r}) \right] , \end{aligned} \tag{36}$$

where in the last step we used (33). If the right-hand side of the previous equation is different from zero, we have $n \neq n'$, from which the Runge-Gross theorem follows. We will prove this last assertion by *reductio ad absurdum*. Assume that $\nabla \cdot \left[n^0(\boldsymbol{r}) \nabla u_k(\boldsymbol{r}) \right] = 0$ with $u_k(\boldsymbol{r}) \neq$ const. [cf. hypothesis (29)], and look at the integral (obtained using Green's theorem)

$$\begin{aligned} \int \mathrm{d}^3 r \, n^0(\boldsymbol{r}) \left[\nabla u_k(\boldsymbol{r}) \right]^2 = &- \int \mathrm{d}^3 r \, u_k(\boldsymbol{r}) \nabla \cdot \left[n^0(\boldsymbol{r}) \nabla u_k(\boldsymbol{r}) \right] \\ &+ \int_{\mathrm{S}} n^0(\boldsymbol{r}) u_k(\boldsymbol{r}) \nabla u_k(\boldsymbol{r}) \cdot d\boldsymbol{S} \, . \end{aligned} \tag{37}$$

The first term on the right-hand side is zero by assumption, while the second term vanishes if the density and the function $u_k(\boldsymbol{r})$ go to zero when $r \to \infty$. This situation is always true for finite systems. Furthermore, as the integrand $n^0(\boldsymbol{r}) \left[\nabla u_k(\boldsymbol{r}) \right]^2$ is always positive, either the density $n^0(\boldsymbol{r})$ or $\nabla u_k(\boldsymbol{r})$ has to vanish identically. The first possibility is obviously ruled out, while the second contradicts our initial assumption that $u_k(\boldsymbol{r})$ is not a constant. This concludes the proof of the Runge-Gross theorem.

2˙2.2. Causality and the quantum mechanical action. In static quantum mechanics, the ground-state of a system can be obtained by minimizing the total energy functional

$$E[\Phi] = \langle \Phi | \, \hat{H} \, | \Phi \rangle \, , \tag{38}$$

where Φ is an N-body function defined in some convenient space. In time-dependent systems there can be no variational principle in terms of the total energy, for this is not a conserved quantity. It is, however, possible to cast the solution of the time-dependent Schrödinger equation into a variational problem using the quantum-mechanical action

$$\mathcal{A}[\Phi] = \int_{t_0}^{t_1} \mathrm{d}t \; \langle \Phi(t) | \, \mathrm{i} \frac{\partial}{\partial t} - \hat{H}(t) \, | \Phi(t) \rangle \, . \tag{39}$$

It is easy to obtain two important properties of the action from its definition (39): i) From the variational equation

$$\frac{\delta \mathcal{A}[\Phi]}{\delta \langle \Phi(t) |} = 0 \tag{40}$$

we recover the time-dependent Schrödinger equation. The function $\Psi(t)$ that makes the functional stationary will therefore be the solution of the time-dependent many-body Schrödinger equation. ii) The action vanishes at the solution point, i.e., $\mathcal{A}[\Psi] = 0$. This is, however, *not* necessarily the minimum value of the action.

In their seminal paper, Runge and Gross offered a derivation of the time-dependent Kohn-Sham equations starting from the action (39)[7]. However, it was later discovered that this approach encompasses two fundamental problems. i) Response functions that stem from (39) are not causal[26, 27]. ii) To derive the variational equation one must impose two independent boundary conditions, namely $\delta\Psi(t_0) = \delta\Psi(t_1) = 0$. It turns out that in TDDFT these two conditions are not independent, for the value of $\delta\Psi(t_1)$ is determined by $\delta\Psi(t_0) = 0$[28, 29]. These two problems were solved by van Leeuwen in 1998[28]. The causality problem is circumvented by the use of the Keldysh formalism[30], while the second problem is resolved by introducing a new action functional that does not contain explicitly $\partial/\partial t$

$$A[n] = -\mathrm{i} \ln \langle \Psi(t_0)| \hat{U}(\tau_f, \tau_i) |\Psi(t_0)\rangle + \int_C \mathrm{d}t \int \mathrm{d}^3 r \, n(\boldsymbol{r}, \tau) v(\boldsymbol{r}, \tau) \,, \tag{41}$$

where τ stands for the Keldysh pseudo-time, $\int_C \mathrm{d}t$ is a shortcut for $\int \mathrm{d}\tau \; \mathrm{d}t/\mathrm{d}\tau$, and U is the evolution operator of the system

$$\hat{U}(\tau_f, \tau_i) = \hat{T}_C \exp\left[-\mathrm{i} \int_{C\ \tau_i}^{\tau_f} \mathrm{d}t \; \hat{H}(\tau)\right] . \tag{42}$$

In the last expression, $\hat{T}_C$ denotes ordering in τ. Response functions calculated from the action (41) will be time-ordered in Keldysh pseudo-time, but properly causal in real time. We will use the action functional (41) to construct a Kohn-Sham system for the time-dependent case.

2˙2.3. Time dependent Kohn-Sham equations. The Runge-Gross theorem asserts that all observables of the quantum mechanical system can be obtained from the density. Nothing is however stated on how to calculate that quantity. For that purpose, we construct an auxiliary system of non-interacting electrons – the Kohn-Sham system. As in the static case, we proceed from now on with the explicitly spin-dependent version of TDDFT which was first formulated by Liu and Vosko[31]. The corresponding time-dependent Kohn-Sham equations are

$$\mathrm{i} \frac{\partial}{\partial t} \varphi_{i\sigma}(\boldsymbol{r}, t) = \hat{H}^{\mathrm{KS}}_{\sigma}(\boldsymbol{r}, t) \varphi_{i\sigma}(\boldsymbol{r}, t) \,, \tag{43}$$

where the Kohn-Sham Hamiltonian is defined as

$$\hat{H}^{\mathrm{KS}}_{\sigma}(\boldsymbol{r}, t) = -\frac{\nabla^2}{2} + v^{\mathrm{KS}}_{\sigma}[n_\uparrow, n_\downarrow](\boldsymbol{r}, t) \,. \tag{44}$$

The potential $v_\sigma^{\rm KS}[n_\uparrow, n_\downarrow](\boldsymbol{r}, t)$ is chosen such that the spin densities of the Kohn-Sham system,

$$n_\sigma(\boldsymbol{r}, t) = \sum_i^{N_\sigma} |\varphi_{i\sigma}(\boldsymbol{r}, t)|^2 \,, \tag{45}$$

equal to the spin densities of the interacting system we want to study. As in ground-state DFT, the time-dependent Kohn-Sham potential is normally written as the sum of three terms [cf. eq. (5)]

$$v_\sigma^{\rm KS}[n_\uparrow, n_\downarrow](\boldsymbol{r}, t) = v_\sigma(\boldsymbol{r}, t) + \int \mathrm{d}^3 r' \, \frac{n(\boldsymbol{r}', t)}{|\boldsymbol{r} - \boldsymbol{r}'|} + v_\sigma^{\rm xc}[n_\uparrow, n_\downarrow](\boldsymbol{r}, t) \,. \tag{46}$$

The first term is the external potential felt by the electrons, while the Hartree potential takes into account the classical electrostatic interaction between the electrons. The third term in (46), the so-called xc potential, includes all non-trivial many-body effects. It can be written as a functional derivative

$$v_\sigma^{\rm xc}(\boldsymbol{r}, t) = \left. \frac{\delta A_{\rm xc}[n_\uparrow, n_\downarrow]}{\delta n_\sigma(\boldsymbol{r}, \tau)} \right|_{n_\sigma = n_\sigma(\boldsymbol{r}, t)} \,, \tag{47}$$

where the xc part of the action is defined by

$$A[n_\uparrow, n_\downarrow] = A_{\rm KS}[n_\uparrow, n_\downarrow] - A_{\rm xc}[n_\uparrow, n_\downarrow] - \frac{1}{2} \int_C \mathrm{d}t \int \mathrm{d}^3 r \int \mathrm{d}^3 r' \, \frac{n(\boldsymbol{r}, \tau) n(\boldsymbol{r}', \tau)}{|\boldsymbol{r} - \boldsymbol{r}'|} \,, \tag{48}$$

where $A_{\rm KS}$ is the action functional (41) written for the Kohn-Sham system.

2˙3. *Time-dependent exchange-correlation potentials*. – In contrast to ground-state DFT, where a plethora of approximations to the xc functional exist (see Sect. **1**˙3), the development of time-dependent xc potentials is still in its infancy. The simplest, and perhaps most widely used, functional is the adiabatic local (spin-) density approximation (ALDA)

$$v_\sigma^{\text{xc ALDA}}(\boldsymbol{r}, t) = \left. \frac{\partial}{\partial n_\sigma} \left[n \, \varepsilon_{\rm xc}^{\rm unif}(n_\uparrow, n_\downarrow) \right] \right|_{n_\alpha = n_\alpha(\boldsymbol{r}, t)} \,. \tag{49}$$

The ALDA potential is nothing more than the ground-state LDA potential evaluated at each time with the density $n_\sigma(\boldsymbol{r}, t)$. This functional is clearly local in space (like the ground-state LDA), and in time.

Following the same reasoning, it is simple to recycle other ground-state xc potentials for use in TDDFT. In general, we can write

$$v_\sigma^{\text{xc adiabatic}}[n_\uparrow, n_\downarrow](\boldsymbol{r}, t) = \tilde{v}_\sigma^{\rm xc}[n_\uparrow, n_\downarrow](\boldsymbol{r})|_{n_\alpha = n_\alpha(\boldsymbol{r}, t)} \,, \tag{50}$$

where $\tilde{v}_{\rm xc}[n_\uparrow, n_\downarrow]$ is some given *ground-state* xc functional. Clearly, $v_\sigma^{\rm xc\ adiabatic}[n_\uparrow, n_\downarrow](\boldsymbol{r}, t)$ is local in time (although it may be non-local in space). Naturally, the adiabatic potential will retain all the problems already present in $\tilde{v}_{\rm xc}[n_\uparrow, n_\downarrow]$. For example, the ALDA potential (as well as most adiabatic GGAs and MGGAs) has the same incorrect asymptotic behavior as the LDA potential (see Sect. **1**˙3).

A functional that does exhibit the correct asymptotic behavior is the EXX. The EXX action is obtained by expanding $A_{\rm xc}$ to first order in e^2 (where e denotes the electron charge)[28, 32]

$$A_{\rm x}^{\rm EXX} = -\frac{1}{2}\sum_\sigma \sum_{j,k}^{\rm occ} \int_C {\rm d}t \int {\rm d}^3 r \int {\rm d}^3 r' \, \frac{\varphi_{j\sigma}^*(\boldsymbol{r}', \tau)\varphi_{k\sigma}(\boldsymbol{r}', \tau)\varphi_{j\sigma}(\boldsymbol{r}, \tau)\varphi_{k\sigma}^*(\boldsymbol{r}, \tau)}{|\boldsymbol{r} - \boldsymbol{r}'|} \,. \tag{51}$$

The EXX is an example of an orbital dependent functional. For this class of action functionals the calculation of the corresponding potential has to be performed through a series of chain rules[21, 22]. First, we use the Runge-Gross theorem to write

$$v_\sigma^{\rm xc}(\boldsymbol{r}, t) = \sum_{\sigma'} \int_C {\rm d}t' \int {\rm d}^3 r' \, \frac{\delta A_{\rm xc}}{\delta v_{\sigma'}^{\rm KS}(\boldsymbol{r}', \tau')} \frac{\delta v_{\sigma'}^{\rm KS}(\boldsymbol{r}', \tau')}{\delta n_\sigma(\boldsymbol{r}, \tau)} \,. \tag{52}$$

The second functional derivative on the right-hand side can be easily identified with the inverse of the Kohn-Sham response function, $\chi_{\rm KS}$ (see Sect. **2**˙4.1). Multiplying by $\chi_{\rm KS}$ and applying the chain rule a second time we arrive at

$$\begin{aligned} &\sum_{\sigma'} \int_C {\rm d}t' \int {\rm d}^3 r' \, \chi_{\sigma\sigma'}^{\rm KS}(\boldsymbol{r}\tau, \boldsymbol{r}'\tau') v_{\sigma'}^{\rm xc}(\boldsymbol{r}', t') = \\ &\sum_{j\sigma'} \int_C {\rm d}t' \int {\rm d}^3 r' \left[\frac{\delta A_{\rm xc}}{\varphi_{j\sigma'}(\boldsymbol{r}'\tau')} \frac{\varphi_{j\sigma'}(\boldsymbol{r}'\tau')}{\delta v_\sigma^{\rm KS}(\boldsymbol{r}, \tau)} + \frac{\delta A_{\rm xc}}{\varphi_{j\sigma'}^*(\boldsymbol{r}'\tau')} \frac{\varphi_{j\sigma'}^*(\boldsymbol{r}'\tau')}{\delta v_\sigma^{\rm KS}(\boldsymbol{r}, \tau)} \right] . \end{aligned} \tag{53}$$

The functional derivative of $A_{\rm xc}$ with respect to the orbitals can be calculated directly, while $\delta\varphi_{j\sigma'}(\boldsymbol{r}'\tau')/\delta v_\sigma^{\rm KS}(\boldsymbol{r}, \tau)$ is obtained from first-order perturbation theory. Rearranging the terms and transforming back to physical time yields the integral equation[32]

$$\sum_j^{\rm occ} \int {\rm d}t' \int {\rm d}^3 r' \, \left[v_\sigma^{\rm xc}(\boldsymbol{r}', t') - u_{j\sigma}^{\rm xc}(\boldsymbol{r}', t') \right] \varphi_{j\sigma}(\boldsymbol{r}, t)\varphi_{j\sigma}^*(\boldsymbol{r}', t') G_\sigma^{\rm R}(\boldsymbol{r}t, \boldsymbol{r}'t') + {\rm c.c.} = 0 \,, \tag{54}$$

where we have defined the retarded Green's function by

$${\rm i}\, G_\sigma^{\rm R}(\boldsymbol{r}t, \boldsymbol{r}'t') = \theta(t - t') \sum_{k=1}^{\infty} \varphi_{k\sigma}^*(\boldsymbol{r}, t)\varphi_{k\sigma}(\boldsymbol{r}', t') \,, \tag{55}$$

and the quantity $u_{j\sigma}^{\mathrm{xc}}$ by

$$u_{j\sigma}^{\mathrm{xc}}(\boldsymbol{r},t) = \frac{1}{\varphi_{j\sigma}^{*}(\boldsymbol{r},t)} \left.\frac{\delta A^{\mathrm{xc}}[\varphi_{j\sigma}]}{\delta\varphi_{j\sigma}(\boldsymbol{r},\tau)}\right|_{\varphi_{j\sigma}=\varphi_{j\sigma}(\boldsymbol{r},t)} . \tag{56}$$

Note that the v_{xc} is still a local potential in space and time, even if it is obtained from the solution of an extremely non-local and non-linear integral equation. The numerical implementation of (54) turns out to be an extremely demanding task. It is, however, possible to obtain an approximate semi-analytical solution of (54) by performing a transformation similar to the one proposed by Krieger, Lee and Iafrate (KLI) for the static case[33, 34, 32]. The KLI potential retains the correct asymptotic behavior of $v_{\mathrm{x}}^{\mathrm{EXX}}$, but becomes local in the time coordinate.

Most of the xc potentials we have presented so far are local in the time coordinate. In 1997 Dobson *et al.* tried to go beyond this limitation by constructing an xc potential with "memory"[35]. They assumed that, in the electron liquid, memory resides not with each fixed point $\boldsymbol{r}$, but rather within each separate "fluid element". Thus the element which arrives at location $\boldsymbol{r}$ at time t "remembers" what happened to it at earlier times when it was at locations different from its present location $\boldsymbol{r}$. Furthermore, the functional satisfies both Galilean invariance[36] and Ehrenfest's theorem. Unfortunately, the numerical implementation of this functional is quite complicated, and no practical applications have appeared to date.

2˙4. *Linear response theory.* – One of the most important applications of TDDFT is the calculation of linear absorption spectra. In this case, the external time-dependent field (the electromagnetic field) is "weak", so we can use linear-response theory to circumvent the solution of the time-dependent Kohn-Sham equations.

2˙4.1. The response function. Let us assume that a system is in its ground state, described by the many-body wave-function $|\Psi_0\rangle$. At $t = t_0$ we perturb the system by applying a (infinitesimally) small time-dependent perturbation, $\delta v_\sigma(\boldsymbol{r},t)$. The linear change in the density is then

$$\delta n_\sigma(\boldsymbol{r},t) = \sum_{\sigma'} \int \mathrm{d}t' \int \mathrm{d}^3 r'\, \chi_{\sigma\sigma'}(\boldsymbol{r}t,\boldsymbol{r}'t')\delta v_{\sigma'}(\boldsymbol{r}',t') . \tag{57}$$

The function χ is the so-called linear density-density response function. A simple calculation shows that χ can be written as the expectation value of the commutator of two density operators[37, 38]

$$\mathrm{i}\chi_{\sigma\sigma'}(\boldsymbol{r}t,\boldsymbol{r}'t') = \theta(t-t') \left\langle\Psi_0\right| \left[\hat{n}_\sigma^H(\boldsymbol{r},t), \hat{n}_{\sigma'}^H(\boldsymbol{r}',t')\right] \left|\Psi_0\right\rangle , \tag{58}$$

where $\hat{n}^H$ is the density operator in the Heisenberg representation. Note that the factor $\theta(t-t')$ ensures that the response function is properly causal. By inserting the completeness relation $1 = \sum_m |\Psi_m\rangle \langle\Psi_m|$ into (58) and Fourier transforming into frequency

space we obtain the Lehmann representation of the density response function

(59)
$$\chi_{\sigma\sigma'}(\boldsymbol{r},\boldsymbol{r}',\omega) = \lim_{\eta\to 0^+}\sum_m \left[\frac{\langle 0|\,\hat{n}_\sigma(\boldsymbol{r})\,|m\rangle\,\langle m|\,\hat{n}_{\sigma'}(\boldsymbol{r}')\,|0\rangle}{\omega-(E_m-E_0)+\mathrm{i}\eta} - \frac{\langle 0|\,\hat{n}_{\sigma'}(\boldsymbol{r}')\,|m\rangle\,\langle m|\,\hat{n}_\sigma(\boldsymbol{r})\,|0\rangle}{\omega+(E_m-E_0)+\mathrm{i}\eta}\right],$$

where η is a small positive infinitesimal, and E_m is the energy of the mth many-body state. This representation is particularly elucidative: as a function of frequency, χ will have poles at the true excitation energies of the system, $\Omega = E_m - E_0$. To find these excitation energies we can therefore search for the poles of χ.

Expression (59) can be quite simplified if the system is non-interacting. In this case, only a few Slater determinants $\langle\Psi_m|$ contribute to χ_s. These involve the excitation of a single particle from an occupied state to an unoccupied state. The non-interacting response function then reads

$$\chi^s_{\sigma\sigma'}(\boldsymbol{r},\boldsymbol{r}',\omega) = \delta_{\sigma\sigma'}\sum_{jk}^{\infty}(f_{k\sigma}-f_{j\sigma})\,\frac{\varphi_{j\sigma}(\boldsymbol{r})\varphi^*_{j\sigma}(\boldsymbol{r}')\varphi_{k\sigma}(\boldsymbol{r}')\varphi^*_{k\sigma}(\boldsymbol{r})}{\omega-(\epsilon_{j\sigma}-\epsilon_{k\sigma})+\mathrm{i}\eta}\,, \tag{60}$$

where $f_{k\sigma}$ denotes the occupation of the state $k\sigma$. As expected, χ_s has poles at the difference of the single-particle eigenvalues, $\epsilon_{j\sigma}-\epsilon_{k\sigma}$, which are the excitation energies in the non-interacting system.

TDDFT provides a very elegant method to evaluate the response function for the interacting system. By construction, the time-dependent Kohn-Sham system has the same density as the interacting system. We can therefore calculate the linear change of the density using the Kohn-Sham electrons

$$\delta n_\sigma(\boldsymbol{r},t) = \sum_{\sigma'}\int\mathrm{d}t'\int\mathrm{d}^3r'\,\chi^\mathrm{KS}_{\sigma\sigma'}(\boldsymbol{r}t,\boldsymbol{r}'t')\delta v^\mathrm{KS}_{\sigma'}(\boldsymbol{r}',t')\,. \tag{61}$$

Note that the Kohn-Sham system is a non-interacting system of electrons, so its response function, χ_KS, will have the form (60). Using the definition of the Kohn-Sham potential, equation (46), we can deduce

$$\delta v^\mathrm{KS}_\sigma(\boldsymbol{r},t) = \delta v_\sigma(\boldsymbol{r},t) + \int\mathrm{d}^3r'\,\frac{\delta n(\boldsymbol{r}',t)}{|\boldsymbol{r}-\boldsymbol{r}'|} + \sum_{\sigma'}\int\mathrm{d}t'\int\mathrm{d}^3r'\,f^\mathrm{xc}_{\sigma\sigma'}(\boldsymbol{r}t,\boldsymbol{r}'t')\delta n_{\sigma'}(\boldsymbol{r}',t')\,, \tag{62}$$

where we have introduced the xc kernel

$$f^\mathrm{xc}_{\sigma\sigma'}[n^\mathrm{GS}_\uparrow,n^\mathrm{GS}_\downarrow](\boldsymbol{r},\boldsymbol{r}',t-t') = \left.\frac{\delta v^\mathrm{xc}_\sigma[n_\uparrow,n_\downarrow](\boldsymbol{r},t)}{\delta n_{\sigma'}(\boldsymbol{r}',t')}\right|_{n_\alpha=n^\mathrm{GS}_\alpha}\,, \tag{63}$$

where the functional derivative is evaluated at the ground-state density, $n^\mathrm{GS}_\alpha(\boldsymbol{r})$. Com-

bining the previous results, we can obtain a Dyson-like equation for the response function

$$\chi_{\sigma\sigma'}(\boldsymbol{r}t,\boldsymbol{r}'t') = \chi^{\mathrm{KS}}_{\sigma\sigma'}(\boldsymbol{r}t,\boldsymbol{r}'t') + \sum_{\alpha\alpha'}\int \mathrm{d}^3x \int \mathrm{d}^3x' \int \mathrm{d}\tau \int \mathrm{d}\tau' \chi^{\mathrm{KS}}_{\sigma\alpha}(\boldsymbol{r}t,\boldsymbol{x},\tau)\left[\frac{\delta(\tau-\tau')}{|\boldsymbol{x}-\boldsymbol{x}'|} + f^{\mathrm{xc}}_{\alpha\alpha'}(\boldsymbol{x}\tau,\boldsymbol{x}'\tau')\right]\chi_{\alpha'\sigma'}(\boldsymbol{x}'\tau',\boldsymbol{r}'t') \,. \tag{64}$$

The previous equation is a formally *exact* representation of the density response of the interacting system. We note that by taking $f_{\mathrm{xc}} = 0$ we recover the random phase approximation (RPA) to the response function.

2˙4.2. The poles of the response function. The response equation is an integral equation that has to be solved self-consistently. Furthermore, one of the ingredients of (64) is the Kohn-Sham response function, χ_{KS}, which is usually obtained though a sum over all (occupied and unoccupied) states [cf. eq. (60)]. This summation usually converges quite slowly and requires the inclusion of many unoccupied states. However, for a system with a discrete spectrum of excitations it is possible to transform (64) into an eigenvalue equation for the excitation energies that circumvents these problems[39, 40, 41].

By writing (64) in frequency space and rearranging the terms, we can obtain the fairly suggestive equation

$$\sum_{\sigma'}\int \mathrm{d}^3r' \,\left[\delta(\boldsymbol{r}-\boldsymbol{r}')\delta_{\sigma\sigma'} - \Xi_{\sigma\sigma'}(\boldsymbol{r},\boldsymbol{r}',\omega)\right]\chi_{\sigma'\sigma''}(\boldsymbol{r}',\boldsymbol{r}'',\omega) = \chi^{\mathrm{KS}}_{\sigma\sigma''}(\boldsymbol{r},\boldsymbol{r}'',\omega)\,, \tag{65}$$

where the function Ξ is defined by

$$\Xi_{\sigma\sigma'}(\boldsymbol{r},\boldsymbol{r}',\omega) = \sum_{\sigma''}\int \mathrm{d}^3r''\,\chi^{\mathrm{KS}}_{\sigma\sigma''}(\boldsymbol{r},\boldsymbol{r}'',\omega)\left[\frac{1}{|\boldsymbol{r}''-\boldsymbol{r}'|} + f^{\mathrm{xc}}_{\sigma''\sigma'}(\boldsymbol{r}'',\boldsymbol{r}',\omega)\right]. \tag{66}$$

As noted in the previous section, the interacting response function, χ, has poles at the true excitation energies of the system, Ω, while the Kohn-Sham response function has poles at the difference of Kohn-Sham eigenvalues. For the equality (65) to hold, it is therefore required that the operator $\delta(\boldsymbol{r}-\boldsymbol{r}')\delta_{\sigma\sigma'} - \Xi$ has zero eigenvalues at the excitation energies Ω, i.e., $\lambda(\omega) \to 1$ when $\omega \to \Omega$, where $\lambda(\omega)$ is the solution of the eigenvalue equation

$$\sum_{\sigma'}\int \mathrm{d}^3\boldsymbol{r}'\,\Xi_{\sigma\sigma'}(\boldsymbol{r},\boldsymbol{r}',\omega)\xi_{\sigma'}(\boldsymbol{r}',\omega) = \lambda(\omega)\xi_{\sigma}(\boldsymbol{r},\omega)\,. \tag{67}$$

Using this equation we can determine the excitation energies of a finite system from the knowledge of χ_{KS} and f_{xc}. After some algebra[42] it is possible to transform (67) into another eigenvalue equation having the true excitation energies as eigenvalues

$$\sum_{j'k'\sigma'}\left[\delta_{jj'}\delta_{kk'}\delta_{\sigma\sigma'}\,\omega_{jk\sigma} + (f_{k'\sigma'} - f_{j'\sigma'})\,K_{jk\sigma,j'k'\sigma'}(\Omega)\right]\beta_{j'k'\sigma'} = \Omega\beta_{jk\sigma}\,, \tag{68}$$

where $\omega_{jk\sigma} = \epsilon_{j\sigma} - \epsilon_{k\sigma}$, and

(69)
$$K_{jk\sigma,j'k'\sigma'}(\omega) = \int \mathrm{d}^3 r \int \mathrm{d}^3 r' \, \varphi^*_{j\sigma}(\boldsymbol{r})\varphi_{k\sigma}(\boldsymbol{r}) \left[\frac{1}{|\boldsymbol{r}-\boldsymbol{r}'|} + f^{\mathrm{xc}}_{\sigma\sigma'}(\boldsymbol{r},\boldsymbol{r}',\omega) \right] \varphi_{j'\sigma'}(\boldsymbol{r}')\varphi^*_{k'\sigma'}(\boldsymbol{r}') \, .$$

If the excitation is well described by a single particle transition, we can neglect the off-diagonal terms of $K_{jk\sigma,j'k'\sigma'}$ to obtain the single-pole approximation (SPA) to the excitation energies[39]. For a spin-unpolarized system it reads

$$\Omega = \omega_{12} + \Re \left[K_{12\uparrow,12\uparrow} \pm K_{12\uparrow,12\downarrow} \right] \, . \tag{70}$$

In the SPA the Coulomb and f_{xc} contributions to the excitation energies appear as a simple additive correction. Furthermore, the SPA is able to describe properly the spin-multiplet structure of an otherwise spin-unpolarized system due to the spin-dependence of the xc kernel.

Several calculations for the lowest excitation energies of atoms and molecules have been performed within this formalism with very promising results[39, 43, 44]. Further results on the SPA, including a discussion on why, and under which circumstances, the SPA is a good approximation can be found in refs. [45, 46].

There is another way of transforming (64) into an eigenvalue equation[40, 41]. The starting point is the parameterization of the linear change of the density

$$\delta n_\sigma(\boldsymbol{r},\omega) = \sum_{ia} \left[\xi_{ia\sigma}(\omega)\varphi^*_{a\sigma}(\boldsymbol{r})\varphi_{i\sigma}(\boldsymbol{r}) + \xi_{ai\sigma}(\omega)\varphi_{a\sigma}(\boldsymbol{r})\varphi^*_{i\sigma}(\boldsymbol{r}) \right] \, , \tag{71}$$

where i labels an occupied and a a virtual state. Inserting this expression in the linear response equation, and after some algebra, it is possible to cast the problem of determining the excitation energies into the pseudo-eigenvalue problem

(72)
$$\sum_{a'i'\sigma'} \left[\delta_{\sigma\sigma'}\delta_{aa'}\delta_{ii'}(\epsilon_{j\sigma} - \epsilon_{k\sigma})^2 + 2\sqrt{\epsilon_{a\sigma} - \epsilon_{i\sigma}} K_{ai\sigma,a'i'\sigma'}(\Omega) \sqrt{\epsilon_{a'\sigma'} - \epsilon_{i'\sigma'}} \right] \beta_{a'i'\sigma'} = \Omega^2 \beta_{ai\sigma} \, .$$

The eigenvalues of this equation are the square of the excitation energies, while the eigenvectors can be used to calculate the oscillator strengths[40, 41].

2˙4.3. Approximations to the exchange-correlation kernel. The xc kernel is an essential ingredient of Kohn-Sham linear response theory, as it includes all non-trivial many-body effects beyond the simple RPA. Furthermore, its functional dependence on the density is *universal*, i.e., f_{xc} is the same for a helium atom, a benzene molecule, or a jellium sphere. It is obviously impossible to obtain the exact xc kernel – it would imply solving the general many-body problem – but several approximations to f_{xc} have appeared in the literature over the years.

A large number of functionals use information about the xc kernel of the uniform electron gas, $f^{\mathrm{unif}}_{\mathrm{xc}}$, to construct an approximate f_{xc} for inhomogeneous systems. As

the electron gas is translationally invariant in space, $f_{\rm xc}^{\rm unif}$ is not a function of $\boldsymbol{r}$ and $\boldsymbol{r}'$ separately, but only depends on their difference, $\boldsymbol{r}-\boldsymbol{r}'$. Moreover, due to translation invariance in time, the xc kernel (both for the electron gas and for inhomogeneous systems) is a function of the difference of times, $t-t'$. In this case, it is often convenient to work in Fourier space, and look at $f_{\rm xc}^{\rm unif}$ as a function of momentum $\boldsymbol{q}$ and frequency ω. Furthermore, the xc kernel of the uniform gas is a *function* of the spin-densities, i.e., $f_{\sigma\sigma'}^{\rm xc\,unif}(\boldsymbol{q},\omega,n_\uparrow,n_\downarrow)$. We will discuss several approximations to this latter quantity in Sect. **2**˙5.2.

The simplest approximation for $f_{\rm xc}$ is the adiabatic local (spin-) density approximation (ALDA)

$$f_{\sigma\sigma'}^{\rm xc\,ALDA}(\boldsymbol{r},\boldsymbol{r}',\omega) = \delta(\boldsymbol{r}-\boldsymbol{r}')f_{\sigma\sigma'}^{\rm xc\,unif}(\boldsymbol{q}\to 0,\omega=0,n_\uparrow,n_\downarrow)\big|_{n_\alpha=n_\alpha(\boldsymbol{r})}\ . \tag{73}$$

The zero momentum limit at zero frequency of the xc kernel for the uniform gas is simply given by

$$\lim_{\boldsymbol{q}\to 0} f_{\sigma\sigma'}^{\rm xc\,unif}(\boldsymbol{q},\omega=0) = \frac{\mathrm{d}^2}{\mathrm{d}n_\sigma \mathrm{d}n_{\sigma'}}\left[n\,\varepsilon_{\rm xc}^{\rm unif}(n_\uparrow,n_\downarrow)\right]\ . \tag{74}$$

Note that the ALDA kernel is local both in time (for it is frequency independent), and in space. Surprisingly, and despite being such a crude approximation, the ALDA approximation yields very good results for a large variety of atoms and molecules (see Sect. **2**˙4.4). In fact, we could expect that the total neglect of the frequency dependence of the kernel would lead to poor excitation energies. This apparent paradox can be understood to some extent by looking at the frequency dependent $f_{\rm xc}$ of the electron gas in the long wave-length limit, $f_{\rm xc}^{\rm unif}(\boldsymbol{q}=0,\omega)$[47]. While the ALDA kernel is a fairly good approximation to $f_{\rm xc}^{\rm unif}(\boldsymbol{q}=0,\omega)$ at low frequency or for systems with high densities, it completely fails to reproduce the strong frequency dependence of $f_{\rm xc}^{\rm unif}(\boldsymbol{q}=0,\omega)$ for low densities (see Sect. **2**˙5.2). The ALDA yields such good excitation energies, even at high frequencies, because excitations at these high frequencies are usually connected to regions of space with a high density of electrons, where the ALDA becomes again a good approximation.

It is straightforward to use the frequency dependent $f_{\rm xc}^{\rm unif}(\boldsymbol{q}=0,\omega)$[47] to construct a dynamical local density approximation (DLDA) to $f_{\rm xc}$ for inhomogeneous systems

$$f_{\sigma\sigma'}^{\rm xc\,DLDA}(\boldsymbol{r},\boldsymbol{r}',\omega) = \delta(\boldsymbol{r}-\boldsymbol{r}')f_{\sigma\sigma'}^{\rm xc\,unif}(\boldsymbol{q}=0,\omega,n_\uparrow,n_\downarrow)\big|_{n_\alpha=n_\alpha(\boldsymbol{r})}\ . \tag{75}$$

This functional was used by Dobson *et al.* to calculate a multipole surface plasmon mode for a neutral Al jellium surface[48]. The shift in frequency of the mode, compared to the usual ALDA results, was about 3%, but there was a 20% increase in the damping.

Several approximations to the xc kernel of the homogeneous electron gas as a function of $\boldsymbol{q}$ have been proposed. This function can also be used to construct an xc kernel for

inhomogeneous systems

$$f^{\rm xc}_{\sigma\sigma'}(\boldsymbol{r},\boldsymbol{r}',\omega) = f^{\rm xc\ unif}_{\sigma\sigma'}(\boldsymbol{r}-\boldsymbol{r}',\omega,n_\uparrow,n_\downarrow)\big|_{n_\alpha=\tilde{n}_\alpha(\boldsymbol{r},\boldsymbol{r}')}\ , \tag{76}$$

with some conveniently chosen function $\tilde{n}_\alpha(\boldsymbol{r},\boldsymbol{r}')$. Now, the problem is which density should be used to evaluate $f^{\rm unif}_{\rm xc}$, or, in other words, how to determine the best function $\tilde{n}$. There are several obvious choices, like $n(\boldsymbol{r})$, $n(\boldsymbol{r}')$, the arithmetic average, $[n(\boldsymbol{r})+n(\boldsymbol{r}')]/2$, the geometrical average, $\sqrt{n(\boldsymbol{r})n(\boldsymbol{r}')}$, etc.

A similar, but simpler, approach is to seek a local density approximation for the response function of the interacting system, rather than merely for the xc kernel. The first step towards such an approximation was given by Chakravarty *et al.*, who proposed the form[49]

$$\chi_{\sigma\sigma'}(\boldsymbol{r},\boldsymbol{r}',\omega) \approx \chi^{\rm unif}_{\sigma\sigma'}(\boldsymbol{r}-\boldsymbol{r}',\omega,n_\uparrow,n_\downarrow)\big|_{n_\alpha=n_\alpha(\boldsymbol{r})}\ , \tag{77}$$

where $\chi_{\rm unif}$ is some suitable approximation to the response function of the homogeneous electron gas. A more symmetric expression was later used to study equations of state for molecular and metallic hydrogen[50]

$$\chi_{\sigma\sigma'}(\boldsymbol{r},\boldsymbol{r}',\omega) \approx \chi^{\rm unif}_{\sigma\sigma'}(\boldsymbol{r}-\boldsymbol{r}',\omega,n_\uparrow,n_\downarrow)\big|_{n_\alpha=\frac{1}{2}[n_\alpha(\boldsymbol{r})+n_\alpha(\boldsymbol{r}')]}\ . \tag{78}$$

Several more complicated approximations have already been tried. For a jellium slab Dobson and Harris found that the best choice was to use the mean-density *ansatz*[51]

$$\tilde{n}_\alpha(z,z') = \frac{1}{z'-z}\int_z^{z'} {\rm d}z'' n_\alpha(z'')\,, \tag{79}$$

where z is the coordinate perpendicular to the slab.

There are other approximations to the xc kernel that do not use information stemming from the electron gas. In 1996 Petersilka *et al.* proposed the kernel[39]

$$f^{\rm x\ PGG}_{\sigma\sigma'}(\boldsymbol{r},\boldsymbol{r}',\omega) = -\delta_{\sigma\sigma'}\frac{1}{|\boldsymbol{r}-\boldsymbol{r}'|}\frac{\left|\sum_k^{\rm occ}\varphi_{k\sigma}(\boldsymbol{r})\varphi^*_{k\sigma}(\boldsymbol{r}')\right|^2}{n_\sigma(\boldsymbol{r})n_\sigma(\boldsymbol{r}')}\,, \tag{80}$$

which can be derived from a simple analytical approximation to the EXX potential[39]. This approximation, called the Slater approximation in the context of Hartree-Fock theory, only retains the leading term in the expression for EXX. The PGG kernel is again frequency independent, but has a rather non-local spatial dependence. Recently, Burke *et al.* proposed to combine the PGG kernel with the ALDA in an attempt to improve excitation energies[52].

Finally, we would like to mention the work by Tokatly and Pankratov, who used a many-body diagrammatic technique to derive an expression for the xc kernel[53]. Moreover, they also showed that spatial non-locality of the xc kernel is strongly frequency dependent, especially in extended systems in the vicinity of the excitation energies.

TABLE I. – $^1\mathrm{S} \rightarrow {}^1\mathrm{P}$ *excitation energies for selected atoms.* Ω_{exp} *denotes the experimental results from [56]. All energies are in hartrees. Table adapted from [39].*

Atom	ω_{LDA}	$\Omega_{\mathrm{LDA/ALDA}}$	ω_{EXX}	$\Omega_{\mathrm{EXX/PGG}}$	Ωexp
Be	0.129	0.200	0.130	0.196	0.194
Mg	0.125	0.176	0.117	0.164	0.160
Ca	0.088	0.132	0.079	0.117	0.108
Zn	0.176	0.239	0.157	0.211	0.213
Sr	0.082	0.121	0.071	0.105	0.099
Cd	0.152	0.214	0.135	0.188	0.199

2˙4.4. Some results for finite systems. Over the years, a vast number of TDDFT calculations for finite systems have been reported in the literature, so only the scantiest of selections can be given here. Before starting our discussion we note that to perform a linear response calculation we need both ground-state Kohn-Sham orbitals, φ_i, and an approximation to f_{xc}. The Kohn-Sham orbitals are usually determined with an approximate v_{xc}. To emphasize this important detail, we will use the notation XXX/YYY, which has the meaning that the ground-state orbitals were calculated with the functional XXX, and that the YYY approximation was used for f_{xc}. It turns out that, for finite systems, the first approximation is in general much more important than the choice of the xc kernel[44, 54].

The first calculation of excitation energies within TDDFT was performed by Zangwill and Soven in 1980[55]. Using the ALDA approximation they obtained excellent results for the photo-absorption cross section of several rare gases for energies just above the ionization threshold.

This good agreement with experiment is not only found in transitions to the continuum. In Table I the $^1\mathrm{S} \rightarrow {}^1$ P excitation energies for several atoms are listed[39]. The agreement of the calculated excitation energies ($\Omega_{\mathrm{LDA/ALDA}}$ and $\Omega_{\mathrm{EXX/PGG}}$) with the experimental results is quite remarkable. We furthermore notice that the EXX/PGG results are superior to the LDA/ALDA. This can be traced back to the quality of the unoccupied states used in the calculations. In contrast to the EXX, the LDA yields unoccupied states that are too extended due to its incorrect asymptotic behavior.

For molecules and clusters, the majority of the TDDFT calculations are performed within the ALDA approximation. The choice of the ALDA has two reasons: i) The ALDA has a very simple analytical expression and is very easy to implement. ii) The results obtained within the ALDA are usually in very good agreement with experimental results, and the use of more sophisticated functionals, like the adiabatic GGAs, does not improve the calculated spectra. In fig. 1 we show an example of such a calculation for the benzene molecule. The agreement with experiment is quite remarkable, especially when looking at the $\pi \rightarrow \pi^*$ resonance at around 7 eV. The spurious peaks that appear in the calculation at higher energies are artifacts caused by an insufficient treatment

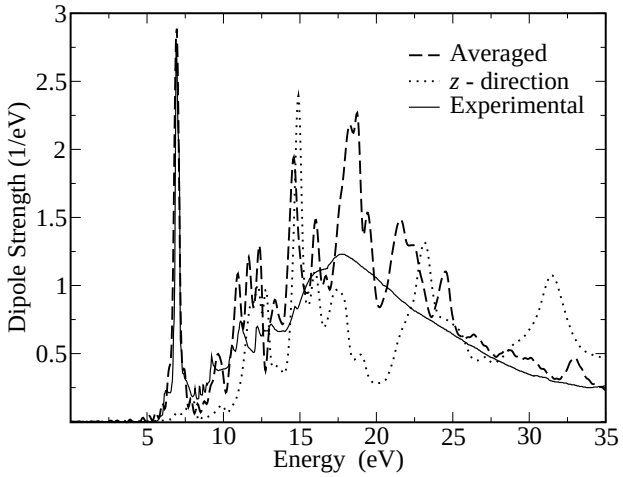

Fig. 1. – Optical absorption of the benzene molecule[57]. Experimental results from ref. [58]. Figure reproduced from ref. [59].

of the unbound states. Other applications of TDLDA that appeared in the literature include small molecules (see e.g., refs. [42, 60]), fullerenes[57, 61, 62], chromophores of proteins[63], etc.

However, and despite its unequivocal success, the application of the ALDA to the calculation of excitation spectra can encounter some difficulties. For example, the ALDA sometimes underestimates the onset of absorption by 1 or 2 eV[54]. Furthermore, some bound excitations will appear in the ALDA as resonances, again due to the wrong asymptotic behavior of the LDA potential. These problems are however solved by using xc potentials with the correct asymptotic behavior, like the van Leeuwen and Baerends GGA[64], the SIC, or the EXX. A more complicated problem is posed by the stretched H_2 molecule, where the ALDA fails to reproduce even qualitatively the shape of the potential curves for the $^3\Sigma_u^+$ and $^1\Sigma_u^+$ states[65, 66]. A detailed analysis of the problem shows that the failure is related to the breakdown of the simple local approximation to the kernel.

2˙4.5. Some results for extended systems. In a extended system, neutral linear excitations can be calculated from the dielectric function, ε. For a spin-compensated system, the dielectric function is related to the response function by the relation

$$\varepsilon^{-1}(\boldsymbol{r}, \boldsymbol{r}', \omega) = \delta(\boldsymbol{r} - \boldsymbol{r}') + \int \mathrm{d}^3x \, \frac{\chi(\boldsymbol{x}, \boldsymbol{r}', \omega)}{|\boldsymbol{r} - \boldsymbol{x}|} \,. \tag{81}$$

In momentum space, ε is a matrix in $\boldsymbol{G}$ and $\boldsymbol{G}'$ (where $\boldsymbol{G}$ is a reciprocal lattice vector) and depends on the wave-vector $\boldsymbol{q}$ (belonging to the first Brillouin zone), i.e, we have

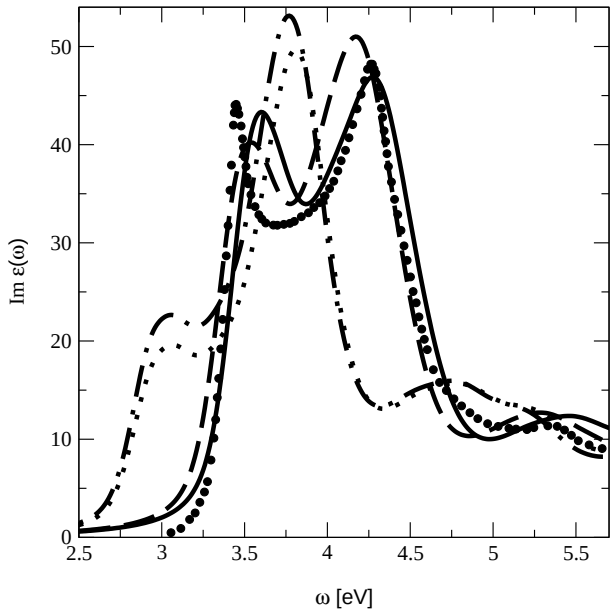

Fig. 2. – Optical absorption spectrum of silicon. In the figure are represented the following spectra: experiment[67] (thick dots), RPA (dotted curve), TDDFT using the ALDA (dot-dashed curve), TDDFT using the RORO kernel[68] (solid curve), and the results obtained from the solution of Bethe-Saltpeter equation (dashed curve). Figure reproduced from ref.[69].

$\varepsilon_{\boldsymbol{G}\boldsymbol{G}'}(\boldsymbol{q})$. Moreover, we define the macroscopic dielectric function, ε_{M}, as the limit

$$\varepsilon_{\mathrm{M}}(\omega) = \lim_{\boldsymbol{q}\to 0} \frac{1}{\varepsilon^{-1}_{\boldsymbol{G}=0,\boldsymbol{G}'=0}(\boldsymbol{q},\omega)} \,. \tag{82}$$

The photo-absorption spectrum can then be obtained from the imaginary part of the macroscopic dielectric function, $\sigma(\omega) = \Im\, \varepsilon_{\mathrm{M}}(\omega)$. Furthermore, the dielectric constant, ε_0, is the value of $\varepsilon_{\mathrm{M}}(\omega)$ at $\omega = 0$.

From an optical absorption experiment we can obtain information about the long-range limit of the dielectric function. There is, however, another spectroscopic technique that probes both the momentum and frequency dependence of ε – electron energy loss spectroscopy (EELS). This technique consists in measuring the energy and momentum of electrons scattered by a sample. The EELS spectrum is obtained from

$$\mathrm{EELS}(\boldsymbol{q},\omega) = -\Im\left[\varepsilon^{-1}_{\boldsymbol{G}=0,\boldsymbol{G}'=0}(\boldsymbol{q},\omega)\right] \,. \tag{83}$$

Several calculations of linear spectra of solids using TDDFT have appeared in the literature. Calculations of the EELS for silicon[69] and diamond[70] using the ALDA are in

quite good agreement with experimental spectra, especially for small $\boldsymbol{q}$. In fact, it turns out that the most important ingredient for the calculation of an EELS spectrum is the proper inclusion of local field effects, while the choice of $f_{\rm xc}$ is relatively unimportant[70]. However, the situation is quite different for the optical absorption spectrum. In fig. 2 we show several calculations of the optical absorption spectrum of Si compared to experimental results. It is clear that the ALDA spectrum is in fairly bad agreement with experiment. Moreover, the ALDA fails to yield any significant improvement over the RPA calculation. This problem can be traced to the behavior of the xc kernel for small $\boldsymbol{q}$: In a semiconductor, $f_{\rm xc}$ should behave asymptotically like $1/q^2$ when $\boldsymbol{q} \to 0$, but $f_{\rm xc}^{\rm ALDA}$, as well as the adiabatic GGAs, approach a finite value.

Several attempts to solve this problem have recently appeared in the literature. For example, using insight gained from the Bethe-Saltpeter equation, Reining *et al.* proposed an $f_{\rm xc}$ of the form $-\alpha/q^2$[68] (the RORO kernel). By taking the empirical value of $\alpha = 0.2$ they were able to describe quite well both the real and imaginary parts of the dielectric constant (see fig. 2). Another approach was followed by Kim and Görling, who calculated the photo-absorption spectrum of silicon using the EXX approximation both in the calculation of the ground-state and for $f_{\rm xc}$[71]. They found that the spectrum collapsed due to the long-range nature of the Coulomb interaction. However, by cutting off the interaction, they were able to obtain results in very good agreement to the experimental curve. We note that these are very recent results, so it is reasonable to expect further developments in the near future.

2˙5. *The exchange-correlation kernel of the homogeneous electron gas.* – As we have seen in Sect. **2**˙4.3 the xc kernel of the homogeneous electron gas is an extremely important ingredient to construct xc functionals for inhomogeneous systems. We will therefore dedicate this section to the study of this important quantity. In a first step we will present several known exact features of $f_{\rm xc}^{\rm unif}$, and then show how these exact features can be incorporated into approximations to the xc kernel of the gas. To simplify the notation we will write all expressions in this section for spin-saturated systems.

2˙5.1. Exact features of $f_{\rm xc}^{\rm unif}$. Several exact features of the xc kernel for the electron gas are easily obtained from the definition (63). As both the external potential and the density are real functions when written in real space and real time, so must be the xc kernel. From this fact one immediately obtains

$$\begin{aligned} \Re f_{\rm xc}^{\rm unif}(\boldsymbol{q},\omega) &= \Re f_{\rm xc}^{\rm unif}(\boldsymbol{q},-\omega)\,, \\ \Im f_{\rm xc}^{\rm unif}(\boldsymbol{q},\omega) &= -\Im f_{\rm xc}^{\rm unif}(\boldsymbol{q},-\omega)\,. \end{aligned} \tag{84}$$

Furthermore, from causality follow the Kramers-Kronig relations:

$$\begin{aligned} \Re f_{\rm xc}^{\rm unif}(\boldsymbol{q},\omega) - f_{\rm xc}^{\rm unif}(\boldsymbol{q},\infty) &= \mathcal{P}\int_{-\infty}^{\infty} \frac{d\omega'}{\pi} \frac{\Im f_{\rm xc}^{\rm unif}(\boldsymbol{q},\omega)}{\omega-\omega'}\,, \\ \Im f_{\rm xc}^{\rm unif}(\boldsymbol{q},\omega) &= -\mathcal{P}\int_{-\infty}^{\infty} \frac{d\omega'}{\pi} \frac{\Re f_{\rm xc}^{\rm unif}(\boldsymbol{q},\omega) - f_{\rm xc}^{\rm unif}(\boldsymbol{q},\infty)}{\omega-\omega'}\,, \end{aligned} \tag{85}$$

where $\mathcal{P}$ denotes the principal value of the integral. Note that, as the infinite frequency limit of the xc kernel is different from zero, one has to subtract $f_{\rm xc}^{\rm unif}(\boldsymbol{q},\infty)$ in the Kramers-Kronig relations.

Several limits of $f_{\rm xc}^{\rm unif}(\boldsymbol{q},\omega)$ are also known. The long wave-length limit at zero frequency, also known as the compressibility sum rule, is given by

$$\lim_{\boldsymbol{q}\to 0} f_{\rm xc}^{\rm unif}(\boldsymbol{q},\omega=0) = \frac{\mathrm{d}^2}{\mathrm{d}n^2}\left[n\varepsilon_{\rm xc}^{\rm unif}(n)\right] \equiv f_0(n)\,, \tag{86}$$

where $\varepsilon_{\rm xc}^{\rm unif}$, the xc energy per particle of the homogeneous electron gas, is known exactly from Monte-Carlo calculations[18]. On the other hand, the infinite frequency limit is

$$\begin{aligned}\lim_{\boldsymbol{q}\to 0} f_{\rm xc}^{\rm unif}(\boldsymbol{q},\omega=\infty) &= -\frac{4}{5}n^{\frac{2}{3}}\frac{\mathrm{d}}{\mathrm{d}n}\left[\frac{\varepsilon_{\rm xc}^{\rm unif}(n)}{n^{2/3}}\right] + 6\,n^{\frac{1}{3}}\frac{\mathrm{d}}{\mathrm{d}n}\left[\frac{\varepsilon_{\rm xc}^{\rm unif}(n)}{n^{1/3}}\right] \\ &\equiv f_\infty(n)\,.\end{aligned} \tag{87}$$

This condition is sometimes called the third frequency moment sum rule. If we insert the best approximations known for $\varepsilon_{\rm xc}^{\rm unif}(n)$ in the previous expressions one can show that the zero frequency limit is always smaller than the infinite frequency limit, and that both these quantities are smaller than zero

$$f_0(n) < f_\infty(n) < 0\,. \tag{88}$$

The behavior of the spin-dependent xc kernel for the electron gas at small $\boldsymbol{q}$ and finite frequency has been studied by Qian *et al.*[72]. Their results show that the long-range expansion has a divergence of the form $\sigma\sigma'/q^2$. However, this divergence cancels out in the density response of spin-compensated systems.

The long wave-length limit of $f_{\rm xc}$ is also known

$$\lim_{\boldsymbol{q}\to\infty} f_{\rm xc}^{\rm unif}(\boldsymbol{q},\omega=0) = c + \frac{b}{q^2}\,, \tag{89}$$

$$\lim_{\boldsymbol{q}\to\infty} f_{\rm xc}^{\rm unif}(\boldsymbol{q},\omega\neq 0) = -\frac{8\pi}{3q^2}\left[1-g(0)\right]\,, \tag{90}$$

where b and c are functions of the density that can be found in ref. [73], and $g(0)$ is the pair-correlation function evaluated at zero distance.

Furthermore, by performing a perturbative expansion of the irreducible polarization to second order in e^2, one finds

$$\lim_{\omega\to\infty} \Im f_{\rm xc}^{\rm unif}(\boldsymbol{q}=0,\omega) = -\frac{23\pi}{15\omega^{3/2}}\,. \tag{91}$$

The real part can be obtained with the help of the Kramers-Kronig relations

$$\lim_{\omega\to\infty} \Re f_{\rm xc}^{\rm unif}(\boldsymbol{q}=0,\omega) = f_\infty(n) + \frac{23\pi}{15\omega^{3/2}}\,. \tag{92}$$

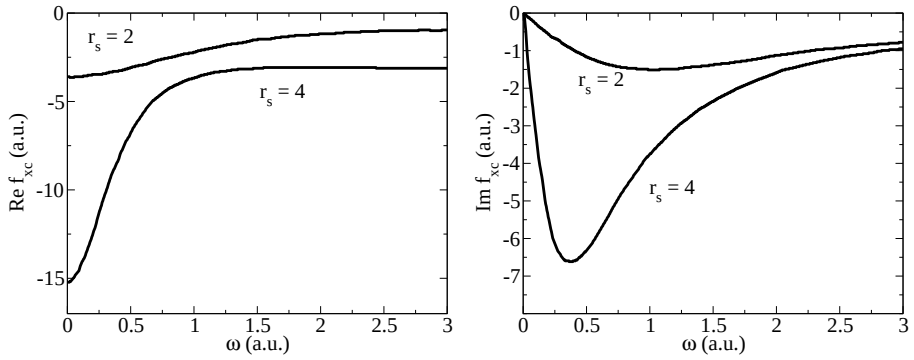

Fig. 3. – Real and imaginary part of the parameterization for $f_{\rm xc}^{\rm unif}(\boldsymbol{q}=0,\omega)$. Figure reproduced from ref. [74].

Normally, in constructing an approximation for the xc kernel of the electron gas one tries to ensure that at least some of these exact features are included in the functional.

2˙5.2. Approximations to $f_{\rm xc}^{\rm unif}$. Innumerous approximations to the xc kernel of the homogeneous electron gas have appeared in the literature in the past decades. The description of all of these is clearly beyond the scope of this review, so we will only present the ones that have been used within the context of TDDFT.

In 1985, Gross and Kohn proposed an analytical form for the long-wavelength limit of the imaginary part of $f_{\rm xc}$ that incorporates several of the limits presented in the previous section[47, 74]

$$\Im f_{\rm xc}^{\rm unif}(\boldsymbol{q}=0,\omega) \approx \frac{\alpha(n)\omega}{[1+\beta(n)\omega^2]^{\frac{5}{4}}}\,. \tag{93}$$

The coefficients α and β are determined using the compressibility sum rule (86) and the third frequency moment sum rule (87). A simple calculation yields

$$\alpha(n) = -A\,[f_\infty(n) - f_0(n)]^{\frac{5}{3}}\,, \tag{94}$$

$$\beta(n) = \quad B\,[f_\infty(n) - f_0(n)]^{\frac{4}{3}}\,, \tag{95}$$

where $A, B > 0$ and independent of n. The real part of $f_{\rm xc}$ can be obtained from the Kramers-Kronig relation

$$\begin{aligned}\Re f_{\rm xc}^{\rm unif}(\boldsymbol{q}=0,\omega) = f_\infty(n) + \frac{2\sqrt{2}\alpha}{\pi\sqrt{\beta}r^2}\Bigg[2E\left(\frac{1}{\sqrt{2}}\right) \\ - \frac{1+r}{2}\Pi\left(\frac{1-r}{2},\frac{1}{\sqrt{2}}\right) - \frac{1-r}{2}\Pi\left(\frac{1+r}{2},\frac{1}{\sqrt{2}}\right)\Bigg]\,,\end{aligned} \tag{96}$$

T

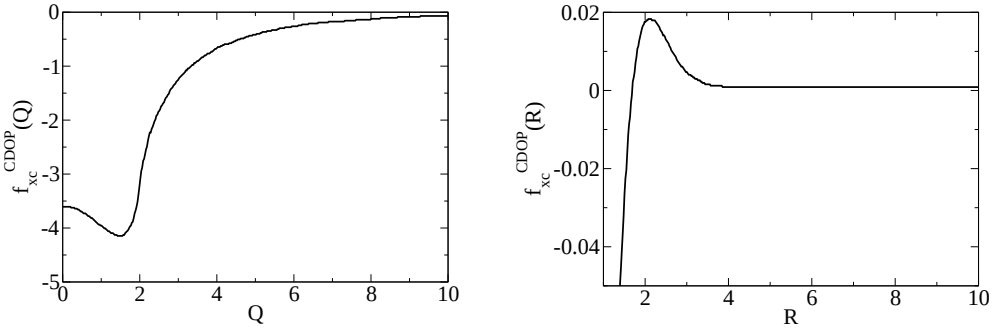

Fig. 4. – The $f_{\rm xc}^{\rm unif\ CDOP}$ plotted in reciprocal and direct space for $r_{\rm s} = 2$ ($Q = q/k_{\rm F}$ and ($R = r\ k_{\rm F}$).

where $r = \sqrt{1+\beta\omega^2}$ and E and Π are the elliptic integrals of second and third kind. In fig. 3 we plotted the real and imaginary part of $f_{\rm xc}^{\rm unif}(\boldsymbol{q}=0,\omega)$ for two different densities, $r_{\rm s} = 2$ and $r_{\rm s} = 4$ ($r_{\rm s}$ is the Wigner-Seitz radius, $1/n = 4\pi r_{\rm s}^3/3$). Both the real and imaginary parts of the xc kernel exhibit a quite strong frequency dependence, especially for the more dilute gas. We note that the ALDA consists in approximating the curves in fig. 3 by their zero frequency limit.

The static ($\omega = 0$) xc kernel for the electron gas as a function of $\boldsymbol{q}$ was calculated by Moroni *et al.* using diffusion Monte-Carlo[73]. Their method is very simple: One perturbs the gas with a static external potential

$$v(\boldsymbol{r}) = 2v_{\boldsymbol{q}}\cos(\boldsymbol{q}\cdot\boldsymbol{r}), \tag{97}$$

which will induce a modulation of the density. The total energy of the gas is then calculated using diffusion Monte-Carlo for a few coupling strengths $v_{\boldsymbol{q}}$, and the static response function is extracted from the expansion

$$E_{\boldsymbol{q}} = E_0 + \frac{\chi(\boldsymbol{q})}{n_0}v_{\boldsymbol{q}}^2 + C_4 v_{\boldsymbol{q}}^4 + \cdots, \tag{98}$$

where $E_{\boldsymbol{q}}$ is the energy (per particle) of the perturbed system, and E_0 and n_0 the energy and density of the unperturbed electron gas. From the response function it is then trivial to extract $f_{\rm xc}^{\rm unif}(\boldsymbol{q},\omega=0)$ by inverting the response equation

$$f_{\rm xc}^{\rm unif}(\boldsymbol{q},\omega=0) = \frac{1}{\chi_{\rm s}(\boldsymbol{q})} - \frac{1}{\chi(\boldsymbol{q})} - \frac{4\pi}{q^2}, \tag{99}$$

where $\chi_{\rm s}(\boldsymbol{q})$ is the response function of the non-interacting electron gas.

Shortly after these calculations, Corradini *et al.* proposed an analytical expression that reproduces the quantum Monte-Carlo data, but also incorporates the known asymptotic behavior for both small and large $\boldsymbol{q}$. The expression of the xc kernel they obtained

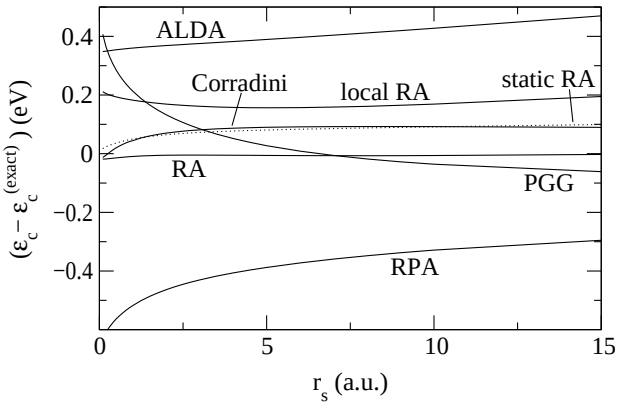

Fig. 5. – Deviation of approximate correlation energies from the "exact" correlation energy per electron of the uniform electron gas[76], as a function of the density. Figure reproduced from ref. [77].

reads, in real space,

(100)
$$f_{\rm xc}^{\rm unif\ CDOP}(x,\omega=0) = -\frac{4\pi C}{k_{\rm F}^2}\delta(x) + \frac{\alpha k_{\rm F}}{4\pi^2\beta}\left(\frac{\pi}{\beta}\right)^{3/2}\left[\frac{k_{\rm F}^2x^2}{2\beta}-3\right]{\rm e}^{-k_{\rm F}^2x^2/4\beta} - B\frac{{\rm e}^{-\sqrt{g}k_{\rm F}x}}{x}\,,$$

where $x = |\boldsymbol{r}-\boldsymbol{r}'|$, $k_{\rm F} = \left(3\pi^2 n\right)^{1/3}$ is the Fermi wave-vector, and B, C, α, β and g are functions of the density. In fig. 4 this kernel is plotted for $r_{\rm s}=2$ in both real and momentum space. Note that this form does not have long-range oscillations, which makes it particularly useful in the calculation of a real solid.

Finally, we would like to mention the approximation of Richardson and Ashcroft (RA) for the xc kernel as a function of momentum, imaginary frequency, and density[75]. Their approach is based on a summation of an infinite class of diagrams within many-body theory. This summation is precise for high densities, but becomes innacurate for sufficiently low densities. To solve this problem, Richardson and Ashcroft proposed a parametrized form that fulfills exactly the compressibility, susceptibility, and the third-frequency moment sum rules at all frequencies, and approaches their many-body results at high densities.

The quality of these kernels was tested by Lein *et al.*, who calculated the correlation energy of the electron gas from the different approximations to $f_{\rm xc}^{\rm unif}$[77]. The ground-state correlation energy can be obtained from the response function at imaginary frequencies and the xc kernel by using the adiabatic connection formula[78, 79]

(101)
$$E_c = -\frac{1}{2\pi}\int {\rm d}^3r \int {\rm d}^3r'\,\frac{1}{|\boldsymbol{r}-\boldsymbol{r}'|}\int_0^1 {\rm d}\lambda \int_0^\infty {\rm d}u\,\left[\chi_\lambda(\boldsymbol{r},\boldsymbol{r}',{\rm i}u) - \chi_{\rm KS}(\boldsymbol{r},\boldsymbol{r}',{\rm i}u)\right]\,,$$

where χ_λ is the response function of a system where the Coulomb interaction between the electrons has been scaled by λ. The results of Lein *et al.* are summarized in fig. 5. While the simple RPA gives an error sometimes as large as 0.5 eV, the ALDA over-corrects the correlation energy by essentially the same amount. The static but $\boldsymbol{q}$ dependent CDOP kernel reduces this error to around 0.1 eV. The error is reduced further (to less than 0.02eV) by using the frequency and momentum dependent RA kernel.

The quality of the RA kernel is further confirmed by the calculations of elementary excitations in the electron gas of Tatarczyk *et al.*[80]. Comparing the calculated plasmon dispersion for $r_\mathrm{s} = 4$ to experimental data for sodium they found that the RA kernel yields results in a very good agreement with experiment, especially at smaller wave-vectors. Although the ALDA correctly reproduces the qualitative features, it deviates significantly from the experimental results, especially at intermediate wave-vectors.

3. – Density functional theory for superconductors

The success of DFT in describing the most varied phenomena in condensed matter physics is unquestionable. However, conventional DFT is not able to describe the superconducting state of matter. In 1988, triggered by the remarkable discovery of the high-T_c materials, Oliveira, Gross and Kohn (OGK) proposed a density functional theory for the superconducting state (SCDFT)[8, 9]. Up to now, the success of SCDFT has been fairly limited, essentially due to the nonexistence of adequate xc functionals. Several recent developments[10, 11, 12] may, however, bring SCDFT to a much wider audience.

In the following we will give an overview of SCDFT, and we will show how to construct an LDA functional that describes the electron-electron part of the interaction. SCDFT is most conveniently formulated using second quantization, so we will use this formulation extensively throughout this section.

3˙1. *Preliminaries.* – The Hamiltonian of a general many-electron system can be written, in second quantization, as

$$\hat{H} = \sum_\sigma \int \mathrm{d}^3 r\, \hat{\psi}^\dagger_\sigma(\boldsymbol{r}) \left[-\frac{\nabla^2}{2} + v(\boldsymbol{r}) - \mu \right] \hat{\psi}_\sigma(\boldsymbol{r}) + \hat{U} + \hat{W}\,, \tag{102}$$

where v is, as usual, the external potential, and μ the chemical potential of the system. Moreover, the term $\hat{U}$ accounts for the Coulomb interaction between the electrons

$$\hat{U} = \frac{1}{2} \sum_{\sigma\sigma'} \int \mathrm{d}^3 r \int \mathrm{d}^3 r'\, \hat{\psi}^\dagger_\sigma(\boldsymbol{r}) \hat{\psi}^\dagger_{\sigma'}(\boldsymbol{r}') \frac{1}{|\boldsymbol{r} - \boldsymbol{r}'|} \hat{\psi}_{\sigma'}(\boldsymbol{r}') \hat{\psi}_\sigma(\boldsymbol{r})\,. \tag{103}$$

To properly describe superconductivity we clearly have to take into account the electron-phonon interaction. In the original OGK formulation this interaction was modeled by a

phonon-mediated effective electron-electron attraction of the form

(104)
$$\hat{W} = -\sum_{\sigma\sigma'}\int \mathrm{d}^3 r_1 \int \mathrm{d}^3 r_2 \int \mathrm{d}^3 r_3 \int \mathrm{d}^3 r_4\, \hat{\psi}^\dagger_\sigma(\boldsymbol{r}_1)\hat{\psi}^\dagger_{\sigma'}(\boldsymbol{r}_2) w(\boldsymbol{r}_1,\boldsymbol{r}_2,\boldsymbol{r}_3,\boldsymbol{r}_4)\hat{\psi}_{\sigma'}(\boldsymbol{r}_3)\hat{\psi}_\sigma(\boldsymbol{r}_4)\,,$$

where w can be a BCS model[81], or a Bardeen-Pines interaction[82], for example. However, this formulation is only able to describe systems where the electron-phonon interaction is weak. More recently, Lüders, starting from a multi-component DFT for the combined electron-nuclear system, extended the OGK formalism to incorporate strong electron-phonon interactions[10].

To the Hamiltonian (102) OGK added the term

$$\hat{\Delta} = -\left[\int \mathrm{d}^3 r \int \mathrm{d}^3 r'\, \Delta_0^*(\boldsymbol{r},\boldsymbol{r}')\hat{\psi}_\uparrow(\boldsymbol{r})\hat{\psi}_\downarrow(\boldsymbol{r}') + \mathrm{H.c.}\right]. \tag{105}$$

This term is only required to break the gauge symmetry of the system, and can be taken to zero at the end of the derivation. Alternatively, it can be viewed as describing a pairing field induced by a nearby superconductor.

3˙2. *Basic theorems.* – The construction of SCDFT follows a parallel route to the derivation of spin-DFT. In this latter theory one uses as basic variables the spin-densities, n_σ, or equivalently, the total density $n = n_\uparrow + n_\downarrow$ and the magnetization density $m = -\mu_0\,(n_\uparrow - n_\downarrow)$. The second density, m, can be viewed as a magnetic order parameter which is zero above a certain critical point and non-zero below, marking the transition from the non-magnetic to the magnetic phase. In a similar way, we will use as basic variables in SCDFT the "normal" density

$$n(\boldsymbol{r}) = \sum_\sigma \left\langle \hat{\psi}^\dagger_\sigma(\boldsymbol{r})\hat{\psi}_\sigma(\boldsymbol{r})\right\rangle, \tag{106}$$

and a non-local, "anomalous" density

$$\chi(\boldsymbol{r},\boldsymbol{r}') = \left\langle \hat{\psi}_\uparrow(\boldsymbol{r})\hat{\psi}_\downarrow(\boldsymbol{r}')\right\rangle. \tag{107}$$

The anomalous density can be viewed as an order parameter that describes the pairing of the electrons, and is zero for any non-superconducting system. With these two densities, it is simple to derive a Hohenberg-Kohn like theorem. By generalizing Mermin's proof for finite temperature DFT[83], OGK proved that[8] "at the temperature $\theta = 1/\beta$, the densities $n(\boldsymbol{r})$ and $\chi(\boldsymbol{r},\boldsymbol{r}')$ in thermal equilibrium determine uniquely the density operator $\hat{\rho} = \mathrm{e}^{-\beta\hat{H}[v,\Delta]}/\mathrm{Tr}\mathrm{e}^{-\beta\hat{H}[v,\Delta]}$, which minimizes the thermodynamic potential $\Omega[v,\Delta] = \mathrm{Tr}\{\hat{\rho}'\hat{H}[v,\Delta] + \theta\hat{\rho}'\ln\hat{\rho}'\}$". The grand-canonical thermodynamic potential can thus be written as a functional of the pair of densities $\{n,\chi\}$

$$\Omega[n,\chi] = F[n,\chi] + \int \mathrm{d}^3 r\, n(\boldsymbol{r})\,[v(\boldsymbol{r}) - \mu] - \int \mathrm{d}^3 r \int \mathrm{d}^3 r'\, \left[\Delta_0^*(\boldsymbol{r},\boldsymbol{r}')\chi(\boldsymbol{r},\boldsymbol{r}') + \mathrm{c.c.}\right]. \tag{108}$$

The functional F is universal, in the sense that its functional dependence on the pair of densities $\{n, \chi\}$ is unique for a given interaction, and does not depend on the external potentials $\{v, \Delta\}$. It is defined by

$$F[n,\chi] = T[n,\chi] + U[n,\chi] + W[n,\chi] - \frac{1}{\beta} S[n,\chi]\,, \tag{109}$$

where $T[n,\chi]$ and $S[n,\chi]$ are the kinetic energy and the entropy functionals of the interacting system, and $U[n,\chi]$ and $W[n,\chi]$ are the density functionals corresponding to the thermal averages of $\hat{U}$ and $\hat{W}$.

As in ordinary DFT, we now introduce a system of non-interacting electrons (the Kohn-Sham system) described by the Hamiltonian

$$\begin{aligned}\hat{H}_{\mathrm{KS}} = \sum_\sigma \int \mathrm{d}^3 r\, \hat{\psi}^\dagger_\sigma(\boldsymbol{r}) \left[-\frac{\nabla^2}{2} + v_{\mathrm{KS}}(\boldsymbol{r}) - \mu \right] \hat{\psi}_\sigma(\boldsymbol{r}) \\ - \left[\int \mathrm{d}^3 r \int \mathrm{d}^3 r'\, \Delta^*_{\mathrm{KS}}(\boldsymbol{r},\boldsymbol{r}') \hat{\psi}_\uparrow(\boldsymbol{r}) \hat{\psi}_\downarrow(\boldsymbol{r}') + \mathrm{H.c.} \right] .\end{aligned} \tag{110}$$

The Kohn-Sham potentials $\{v_{\mathrm{KS}}, \Delta_{\mathrm{KS}}\}$ are chosen such that the pair of densities of the Kohn-Sham system equals the densities of the interacting system, $\{n, \chi\}$. They are given by [cf. eq. (5)]

$$v_{\mathrm{KS}}[n,\chi](\boldsymbol{r}) = v(\boldsymbol{r}) + \int \mathrm{d}^3 r'\, \frac{n(\boldsymbol{r}')}{|\boldsymbol{r}-\boldsymbol{r}'|} + v_{\mathrm{xc}}[n,\chi](\boldsymbol{r})\,, \tag{111a}$$

$$\Delta_{\mathrm{KS}}[n,\chi](\boldsymbol{r},\boldsymbol{r}') = \Delta(\boldsymbol{r},\boldsymbol{r}') - \frac{\chi(\boldsymbol{r},\boldsymbol{r}')}{|\boldsymbol{r}-\boldsymbol{r}'|} + \Delta_{\mathrm{xc}}[n,\chi](\boldsymbol{r},\boldsymbol{r}')\,. \tag{111b}$$

The xc potentials are formally defined as functional derivatives of the xc free-energy functional $F_{\mathrm{xc}}[n,\chi]$

$$v_{\mathrm{xc}}[n,\chi](\mathbf{r}) = \frac{\delta F_{\mathrm{xc}}[n,\chi]}{\delta n(\mathbf{r})}\,, \tag{112a}$$

$$\Delta_{\mathrm{xc}}[n,\chi](\mathbf{r},\mathbf{r}') = -\frac{\delta F_{\mathrm{xc}}[n,\chi]}{\delta \chi^*(\mathbf{r},\mathbf{r}')}\,. \tag{112b}$$

Finally, $F_{\mathrm{xc}}[n,\chi]$ is defined through the expression

$$\begin{aligned}F[n,\chi] = T_{\mathrm{s}}[n,\chi] - \frac{1}{\beta} S_{\mathrm{s}}[n,\chi] + \frac{1}{2} \int \mathrm{d}^3 r \int \mathrm{d}^3 r'\, \frac{n(\boldsymbol{r}) n(\boldsymbol{r}')}{|\boldsymbol{r}-\boldsymbol{r}'|} \\ + \int \mathrm{d}^3 r \int \mathrm{d}^3 r'\, \frac{|\chi(\boldsymbol{r},\boldsymbol{r}')|^2}{|\boldsymbol{r}-\boldsymbol{r}'|} + F_{\mathrm{xc}}[n,\chi]\,.\end{aligned} \tag{113}$$

Note that in the expression (113) we separated out all "trivial" contributions to the free-energy, namely the non-interacting kinetic energy and entropy ($T_{\mathrm{s}}[n,\chi]$ and $S_{\mathrm{s}}[n,\chi]$),

the Hartree term, which takes into account the classical electrostatic interaction between the electrons, and an anomalous Hartree energy. The remainder, which contains all non-trivial many-body contributions to the free-energy, is the xc energy.

The Kohn-Sham equations are then obtained by diagonalizing the Hamiltonian (110). The resulting expression has the familiar form of the Bogoliubov-de Gennes equations[84]

$$\begin{aligned} &\left[-\frac{\nabla^2}{2} + v_{\rm KS}(\boldsymbol{r}) - \mu\right] u_i(\boldsymbol{r}) + \int \mathrm{d}^3 r'\, \Delta_{\rm KS}(\boldsymbol{r},\boldsymbol{r}') v_i(\boldsymbol{r}') = E_i u_i(\boldsymbol{r}) \\ -&\left[-\frac{\nabla^2}{2} + v_{\rm KS}(\boldsymbol{r}) - \mu\right] v_i(\boldsymbol{r}) + \int \mathrm{d}^3 r'\, \Delta^*_{\rm KS}(\boldsymbol{r},\boldsymbol{r}') u_i(\boldsymbol{r}') = E_i v_i(\boldsymbol{r})\,, \end{aligned} \tag{114}$$

where $u_i(\boldsymbol{r})$ and $v_i(\boldsymbol{r})$ are the particle and hole amplitudes. The densities can then be obtained through the relations

$$n(\boldsymbol{r}) = 2\sum_i \left[|u_i(\boldsymbol{r})|^2 f_\beta(E_i) + |v_i(\boldsymbol{r})|^2 f_\beta(-E_i)\right]\,, \tag{115a}$$

$$\chi(\boldsymbol{r},\boldsymbol{r}') = \sum_i \left[u_i(\boldsymbol{r}) v_i^*(\boldsymbol{r}') f_\beta(-E_i) - u_i(\boldsymbol{r}') v_i^*(\boldsymbol{r}) f_\beta(E_i)\right]\,, \tag{115b}$$

where $f_\beta(E_i)$ denotes the Fermi distribution. In 1993, Suvasini, Temmerman and Gyorffy [85] presented the first numerical solution of the above KS equations for niobium with a phenomenological xc functional using a linear muffin-tin orbital (LMTO) method, generalized to solve the Bogoliubov-de Gennes equations. More recently, the first attempts to tackle the high-T_c superconductors within this DFT framework have appeared [86, 87]. In this work, the xc functional was modeled by a phenomenological interaction kernel which was expanded in the LMTOs of a recently proposed eight-band model for YBCO[88, 89]. The expansion coefficients $K_{RL,R'L'}$ characterizing the effective interaction between orbital L at site R with orbital L' at site R' were treated as adjustable parameters. The comparison of various scenarios pointed to the conclusion that the pairing mechanism operates between electrons of opposite spins on nearest-neighbor Cu sites.

While it is certainly fruitful to study the xc potential of a particular system, the charm and the power of DFT derives from the *universality* of the xc functional: One and the same functional of n and χ should predict the specific properties of *all* materials. Although a wealth of xc functionals exists for normal DFT, the case is quite different in the case of DFT for superconductors. The only two functionals proposed to date are: i) In 1999, Kurth *et al.* proposed an LDA-type functional[90] which only accounts for the purely electronic correlations in superconductors and is based on the xc energy of a uniform electron gas made superconducting by an external pairing field. To calculate the latter quantity, the authors proposed the use of Kohn-Sham perturbation theory at the level of a random phase approximation (RPA)[91]. ii) More recently, Lüders *et al.* constructed a functional, using a method resembling the optimized-effective potential method, that describes both strong electron-phonon interactions and electron-electron

repulsion[10, 11, 12]. First results for the simple metals calculated with this functional turn out to be in fairly good agreement with experiment[12]. In the following we will present a fairly detailed account of the first of these functionals – the LDA for superconductors.

3˙3. *An LDA for superconductors.* – The LDA functional for superconductors (SCLDA) [90] can be constructed in analogy to the local spin density approximation (LSDA), with the anomalous density playing the role of the spin-magnetization density in the LSDA. The key ingredient of the SCLDA is the xc energy per particle of the uniform gas that turns out to be a *function* of the normal density n, and a *functional* of the anomalous density $\chi(\boldsymbol{r}-\boldsymbol{r}')$, i.e.

$$\varepsilon_{\rm xc}^{\rm unif} = \varepsilon_{\rm xc}^{\rm unif}[n, \chi(\boldsymbol{r}-\boldsymbol{r}')]\,. \tag{116}$$

Various methods can, in principle, be used to obtain $\varepsilon_{\rm xc}^{\rm unif}$, like e.g. quantum Monte-Carlo, or many-body perturbation theory. We will use the latter to write the xc energy of the electron gas as a series expansion in powers of e^2, where e is the electron charge.

3˙3.1. The local spin density approximation. In this section we will make a brief detour and examine the construction of the LSDA. This construction will then serve as a template for the development of the LDA for superconductors.

In the standard formulation of spin DFT the xc energy functional is a *universal* functional of the pair of densities (n, m), i.e., $F_{\rm xc}^{\rm spin\ DFT}[n, m]$. The spin local density approximation (LSDA) to $F_{\rm xc}$ is then defined by

$$F_{\rm xc}^{\rm LSDA}[n(\boldsymbol{r}), m(\boldsymbol{r})] = \int {\rm d}^3 r\, n(\boldsymbol{r})\, \varepsilon_{\rm xc}^{\rm unif}(n, m)\Big|_{\substack{n=n(\boldsymbol{r})\\ m=m(\boldsymbol{r})}} \tag{117}$$

where $\varepsilon_{\rm xc}^{\rm unif}(n, m)$ is the xc energy per particle of an electron-gas of density n, and magnetization m. To evaluate this quantity the electron gas is exposed to a constant magnetic field, B (in the z direction)

$$\hat{H} = \hat{T} + \hat{U} - \int {\rm d}^3 r\, \hat{m}_z(\boldsymbol{r}) B\,, \tag{118}$$

with

$$\hat{m}_z(\boldsymbol{r}) = -\mu_0 \left[\hat{\psi}_\uparrow^\dagger(\boldsymbol{r})\hat{\psi}_\uparrow(\boldsymbol{r}) - \hat{\psi}_\downarrow^\dagger(\boldsymbol{r})\hat{\psi}_\downarrow(\boldsymbol{r})\right]\,. \tag{119}$$

The external magnetic field will produce a finite (and constant) magnetization, m, in the gas, allowing us to calculate $\varepsilon_{\rm xc}^{\rm unif}(n, m)$.

Note that what enters the construction of the LSDA is the xc energy of the uniform gas exposed to a *finite* magnetic field. It is therefore of no relevance that the uniform gas (without a magnetic field) only becomes spin-polarized at very low densities[3].

3˙3.2. Construction of an LDA for superconductors. We now construct the LDA for superconductors (SCLDA) in close analogy to the LSDA. The homogeneous electron gas is exposed to an external pairing field Δ. To preserve the translational invariance of the uniform gas, Δ is chosen to depend on the difference $(\boldsymbol{r}-\boldsymbol{r}')$. As a consequence, the induced order parameter $\chi(\boldsymbol{r},\boldsymbol{r}')$ is translationally invariant as well. It is therefore convenient to work in Fourier space. The Fourier transform of the anomalous density is

$$\chi(\boldsymbol{k}) = \int \mathrm{d}^3 s\, \mathrm{e}^{\mathrm{i}\boldsymbol{k}\boldsymbol{s}} \chi(\boldsymbol{s})\,, \tag{120}$$

where $\boldsymbol{s}=\boldsymbol{r}-\boldsymbol{r}'$ is the relative coordinate of the Cooper pair. (The Fourier transform of the pair potential is defined in a similar way.) The SCLDA is then defined as

$$F_{\mathrm{xc}}^{\mathrm{SCLDA}}[n(\boldsymbol{R}),\chi(\boldsymbol{R},\boldsymbol{k})] = \int \mathrm{d}^3 R\; n(\boldsymbol{R})\, \varepsilon_{\mathrm{xc}}^{\mathrm{unif}}[n,\chi(\boldsymbol{k})]\Big|_{\substack{n=n(\boldsymbol{R})\\ \chi=\chi_W(\boldsymbol{R},\boldsymbol{k})}}\,, \tag{121}$$

where $\boldsymbol{R}$ represents the center of mass of the Cooper pair, $\boldsymbol{R}=(\boldsymbol{r}+\boldsymbol{r}')/2$. The function $\chi_W(\boldsymbol{R},\boldsymbol{k})$ is the Wigner transform of the anomalous density of the inhomogeneous system, given by

$$\chi_W(\boldsymbol{R},\boldsymbol{k}) = \int \mathrm{d}^3 s\, \mathrm{e}^{\mathrm{i}\boldsymbol{k}\boldsymbol{s}} \chi\left(\boldsymbol{R}+\frac{\boldsymbol{s}}{2},\boldsymbol{R}-\frac{\boldsymbol{s}}{2}\right)\,. \tag{122}$$

This expression trivially reduces to the common LDA for non-superconducting systems in the limit $\chi\to 0$. At first sight, other definitions of an LDA for superconductors with the correct non-superconducting limit might be conceivable. However, it can be shown that (121) is the *only* correct definition. This follows from a semi-classical expansion of the total energy[92]. The lowest-order terms in $\hbar$ are identical with the SCLDA[93], leading to equation (121).

3˙3.3. How to calculate $\varepsilon_{\mathrm{xc}}^{\mathrm{unif}}$. The LDA requires $\varepsilon_{\mathrm{xc}}^{\mathrm{unif}}$ as an input. To evaluate this function we use Kohn-Sham perturbation theory. The unperturbed system is described by the Hamiltonian

$$\hat{H}_{\mathrm{KS}} = \sum_{\sigma}\sum_{\boldsymbol{k}}\left(\frac{k^2}{2}-\mu_{\mathrm{KS}}\right)\hat{c}^{\dagger}_{\boldsymbol{k}\sigma}\hat{c}_{\boldsymbol{k}\sigma} - \sum_{k}\left[\Delta^{*}_{\mathrm{KS}}(\boldsymbol{k})\hat{c}_{\boldsymbol{k}\uparrow}\hat{c}_{-\boldsymbol{k}\downarrow} + \mathrm{H.c.}\right]\,, \tag{123}$$

where $\hat{c}_{\boldsymbol{k}\sigma}$ destroys an electron with momentum $\boldsymbol{k}$ and spin σ, μ_{KS} is a shorthand for the constant $(\mu - v_{\mathrm{KS}})$ and $\Delta_{\mathrm{KS}}(\mathbf{k})$ is the KS pairing potential (111b) for a homogeneous system. We then use as perturbation $\hat{H}_1 = \hat{H} - \hat{H}_{\mathrm{KS}}$, where $\hat{H}$ is the many-body OGK Hamiltonian of the homogeneous electron gas. Due to the the presence of the pairing field $\Delta_{\mathrm{KS}}(\mathbf{k})$ in the unperturbed Hamiltonian, $\hat{H}_{\mathrm{KS}}$, the perturbation expansion not only involves the normal Kohn-Sham Green's functions, G_{KS}, but also the anomalous

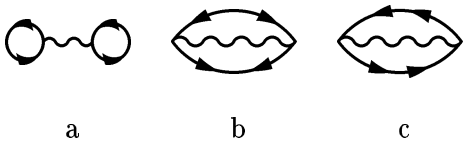

Fig. 6. – First order diagrams contributing to the free energy of the superconducting electron gas.

Kohn-Sham propagators, $F_{\rm KS}$ and $F^\dagger_{\rm KS}$. These anomalous propagators are defined as expectation values of two creation or two annihilation operators

$$F^{\rm KS}_{\sigma\sigma'}(\boldsymbol{r}\tau,\boldsymbol{r}'\tau') = -{\rm Tr}\left\{\hat\rho_{\rm KS}\,\hat T\hat\psi_\sigma(\boldsymbol{r}\tau)\hat\psi_{\sigma'}(\boldsymbol{r}'\tau')\right\}\,, \tag{124a}$$

$$F^{\dagger\,{\rm KS}}_{\sigma\sigma'}(\boldsymbol{r}\tau,\boldsymbol{r}'\tau') = -{\rm Tr}\left\{\hat\rho_{\rm KS}\,\hat T\hat\psi^\dagger_\sigma(\boldsymbol{r}\tau)\hat\psi^\dagger_{\sigma'}(\boldsymbol{r}'\tau')\right\}\,, \tag{124b}$$

where the field operators are written in the Heisenberg picture, $\hat T$ stands for the usual time-ordering operator, which orders the operators from right to left in ascending time order, and the statistical operator $\hat\rho_{\rm KS}$ is defined by

$$\hat\rho_{\rm KS} = \frac{{\rm e}^{-\beta\hat H_{\rm KS}}}{Z_{\rm KS}} = {\rm e}^{\beta(\Omega_{\rm KS}-\hat H_{\rm KS})} \quad ; \quad Z_{\rm KS} = {\rm e}^{-\beta\Omega_{\rm KS}} = {\rm Tr}\,{\rm e}^{-\beta\hat H_{\rm KS}}\,. \tag{125}$$

When drawing Feynman diagrams we will represent the anomalous propagators by lines with arrows pointing in opposite directions, the normal Green's functions by lines with arrows pointing in the same direction, and the bare Coulomb interaction by wiggly lines. The three diagrams contributing to the free energy to first order in $\hat H_1$ are depicted in fig. 6. However, only the third of these diagrams, fig. 6c, contributes to the xc free energy F_{xc}. Figure 6a corresponds to the classical electrostatic energy of the charge distribution, while fig. 6b gives the "anomalous" Hartree energy – both these terms have already been taken into account by eq. (113). Figure 6c is the generalization of the normal exchange energy, and yields

$$n\varepsilon_{\rm x}^{\rm unif} = -\frac{1}{4}\int\frac{{\rm d}^3k}{(2\pi)^3}\int\frac{{\rm d}^3k'}{(2\pi)^3}\frac{4\pi}{|\boldsymbol{k}-\boldsymbol{k}'|^2}\,\left[1-\frac{\xi_k}{E_{\boldsymbol{k}}}\tanh\left(\frac{\beta}{2}E_{\boldsymbol{k}}\right)\right]\left[1-\frac{\xi_{k'}}{E_{\boldsymbol{k}'}}\tanh\left(\frac{\beta}{2}E_{\boldsymbol{k}'}\right)\right]\,, \tag{126}$$

where $E_{\boldsymbol{k}} = \sqrt{\xi_k^2+|\Delta(\boldsymbol{k})|^2}$ and $\xi_k = k^2/2-\mu_{\rm KS}$.

In second order, some of the diagrams are divergent due to the long range of the Coulomb interaction. This is a well known fact, already present in the non-superconducting gas, that can be cured by performing partial resummations of infinite subsets of diagrams. The simplest of these is the random phase approximation (RPA)[91], which includes the most divergent terms in every order, and is exact in the high-density limit.

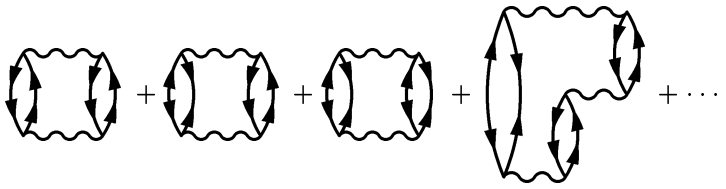

Fig. 7. – The RPA diagrams.

The RPA for superconductors includes all the normal and anomalous bubble diagrams as indicated in fig. 7. The resummation leads to, after evaluating the spin sums,

$$n\varepsilon_{\rm c}^{\rm unif\ RPA} = \frac{1}{2\beta}\sum_{\nu_n}\int\frac{{\rm d}^3q}{(2\pi)^3}\left\{\log\left[1-\Pi_{\rm KS}(\mathbf{q},\nu_n)\frac{4\pi}{q^2}\right]+\Pi_{\rm KS}(\mathbf{q},\nu_n)\frac{4\pi}{q^2}\right\}, \tag{127}$$

with the even Matsubara frequencies $\nu_n = 2n\pi/\beta$. $\Pi_{\rm KS}$ is the irreducible KS polarization given by

$$\begin{aligned}\Pi_{\rm KS}(\mathbf{q},\nu_n) = \frac{2}{\beta}\sum_{\omega_n}\int\frac{{\rm d}^3k}{(2\pi)^3}\Big\{&G_{\rm KS}(\boldsymbol{k},\omega_n)G_{\rm KS}(\boldsymbol{k}+\boldsymbol{q},\omega_n+\nu_n)\\ &+F_{\rm KS}(\boldsymbol{k},\omega_n)F^{\dagger}_{\rm KS}(\boldsymbol{k}+\mathbf{q},\omega_n+\nu_n)\Big\},\end{aligned} \tag{128}$$

with the odd Matsubara frequencies $\omega_n = (2n+1)\pi/\beta$.

To gain some insight in the relative importance of the anomalous Hartree, the exchange and the RPA contributions, we calculated these for a simple s-wave model $\Delta_{\rm KS}(\boldsymbol{k})$,

$$\Delta_{\rm KS}(\boldsymbol{k}) = \mu\,\delta\,{\rm e}^{-\frac{(k/k_{\rm F}-1)^2}{\sigma^2}} \tag{129}$$

where $k_{\rm F}$ is the Fermi wave vector, and δ and σ are (dimensionless) parameters.

The results are summarized in figs. 8, where we show different contributions to the condensation energy per unit volume. (The energy per unit volume is simply the energy per unit particle times the density, $e = n\varepsilon$.) The different curves are: the difference of exchange energies, $e_{\rm x}^{\rm S} - e_{\rm x}^{\rm N}$, in the superconducting (S) and normal (N) states, the negative difference $-(e_{\rm RPA}^{\rm S} - e_{\rm RPA}^{\rm N})$ of the corresponding RPA correlation energies, the anomalous Hartree energy, $e_{\rm AH}$, and the total condensation energy, $e_{\rm cond}$. In the left panel of fig. 8 these energies are plotted versus the parameter δ for $\sigma = 1$, while in the right panel the same quantities are plotted as functions of σ for $\delta = 0.01$. These two plots were obtained for $r_{\rm s} = 1$, and the temperature was set to zero. The dependence of the energies on the parameters σ and δ turns out to be rather smooth. The largest positive contribution comes from the anomalous Hartree term, and is almost canceled by the RPA correlation energy difference $(e_{\rm RPA}^{\rm S} - e_{\rm RPA}^{\rm N})$. The exchange part is positive,

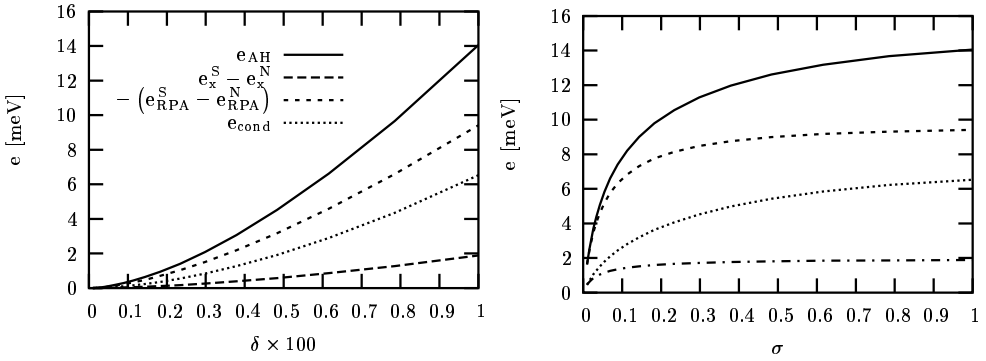

Fig. 8. – Energies versus δ for an s-wave pair-potential with $\sigma = 1$ (left panel), and energies versus σ for a pair-potential with $\delta = 0.01$ (right panel). Both panels were calculated for $r_s = 1$ and $T = 0\,\mathrm{K}$.

but much smaller (almost an order of magnitude) than the other two terms. The same statement holds true for $0.01 \leq \delta \times 100 \leq 1$, $0.01 \leq \sigma \leq 1$ and $r_s = 0.1, 1, 2, 3, 4$, and 5. In the conventional s-wave superconductors, the pairing mechanism is phononic, and the above Coulombic positive-energy contributions reduce superconductivity.

3˙3.4. Construction of the explicit functional. As we have seen, from many-body perturbation theory we obtain the xc free energy as an *explicit* functional of the potentials $\tilde{\varepsilon}_{xc}^{unif}[\mu_{KS}, \Delta_{KS}(\boldsymbol{k})]$. However, in the SCLDA we need the xc free energy of the uniform gas written as a functional of the densities, i.e., $\varepsilon_{xc}^{unif}[n, \chi(\boldsymbol{k})]$. From the Hohenberg-Kohn theorem for superconductors we know that the pair of potentials is in a one-to-one correspondence with the pair of densities, so we can write

$$\mu_{KS} = \mu_{KS}[n, \chi(\boldsymbol{k})]\,, \tag{130a}$$

$$\Delta_{KS}(\boldsymbol{k}) = \Delta_{KS}[n, \chi(\boldsymbol{k})]\,. \tag{130b}$$

The desired density functional can then be written as

$$\varepsilon_{xc}^{unif}\left[n, \chi(\boldsymbol{k})\right] = \tilde{\varepsilon}_{xc}^{unif}\left[\mu_{KS}\left[n, \chi(\boldsymbol{k})\right], \Delta_{KS}\left[n, \chi(\boldsymbol{k})\right]\right] \tag{131}$$

The functionals (130) can be constructed explicitly with the help of relations (115) applied to the uniform electron gas

$$n = \int \frac{\mathrm{d}^3 k}{(2\pi)^3} \left[1 - \frac{\xi_k}{E_{\boldsymbol{k}}} \tanh\left(\frac{\beta}{2} E_{\boldsymbol{k}}\right)\right] \tag{132a}$$

$$\chi(\boldsymbol{k}) = \frac{1}{2} \frac{\Delta_{KS}(\boldsymbol{k})}{E_{\boldsymbol{k}}} \tanh\left(\frac{\beta}{2} E_{\boldsymbol{k}}\right)\,. \tag{132b}$$

In practice, to obtain the potentials $\{\tilde{\mu}_{KS}, \tilde{\Delta}_{KS}(\boldsymbol{k})\}$ given some densities $\{\tilde{n}, \tilde{\chi}(\boldsymbol{k})\}$, we follow the steps:

1. First, invert equation (132b), for the given inverse temperature β, to obtain the relation $\Delta_{\rm KS}(\boldsymbol{k}) = D(\mu_{\rm KS}, \tilde{\chi}(\boldsymbol{k}))$. This mapping can be obtained analytically at zero temperature, but will have to be evaluated numerically otherwise.

2. Insert D into (132a), to obtain the density as a function $n(\mu_{\rm KS})$.

3. Solve numerically the resulting equation, $\tilde{n} = n(\tilde{\mu}_{\rm KS})$, and find $\tilde{\mu}_{\rm KS}$.

4. Insert $\tilde{\mu}_{\rm KS}$ into the inverse function D, to obtain $\tilde{\Delta}_{\rm KS}(\boldsymbol{k}) = D(\tilde{\mu}_{\rm KS}, \tilde{\chi}(\boldsymbol{k}))$.

This concludes the construction of the SCLDA density functional, equation (121). Unfortunately, there were no applications of the SCLDA to real materials up to now.

4. – Conclusions

In this article we reviewed two extensions of ground-state DFT, the first to time-dependent systems (TDDFT), and the second to the phenomenon of superconductivity (SCDFT). The construction of both theories is similar, and follows closely the development of ordinary DFT. The first step is the election of the densities that will be used as basic variables of the theory. In TDDFT one uses the time-dependent density, $n(\boldsymbol{r}, t)$, while in SCDFT the choice falls on the pair of densities $\{n(\boldsymbol{r}), \chi(\boldsymbol{r}, \boldsymbol{r}')\}$. The formal foundations are then given by a Hohenberg-Kohn like theorem and by a Kohn-Sham scheme, where the complexities of the many-body system are cast into the form of xc potentials.

Although several different xc functionals have been proposed over the years, the local density approximations still remain the most widespread. The basic idea behind an LDA is very simple: One assumes that the inhomogeneous system behaves *locally* like a uniform electron gas. This somewhat crude approximation is able to describe quite complex effects. For example, when the LDA is used in the context of TDDFT, it is able to predict very accurately linear response spectra of finite systems. For extended systems the situation is more complicated: although EELS spectra of different materials come out in quite good agreement with experiment, the LDA fails to reproduce the optical absorption spectrum of semiconductors.

Certainly, the development of new, better, xc functionals does not end with the LDA. For ground-state DFT we now have available very accurate GGAs, meta-GGAs, orbital functionals, etc. The variety is not so large for TDDFT and SCDFT, but the pursuit for xc functionals is still an active field of research. However, it is clear that the electron-gas will continue to be one of the most important paradigms in any future development.

5. – Acknowledgements

We would like to thank Angelica Zacarias, Nicole Helbig and Silvana Botti for their useful suggestions and comments during the preparation of the manuscript. This work was supported in part by the Deutsche Forschungsgemeinschaft, the EXC!TiNG Research and Training Network and the NANOQUANTA Network of Excellence.

REFERENCES

[1] WIGNER E., *Phys. Rev.* **46**, 1002 (1934).
[2] KOHN W. and LUTTINGER J. M., *Phys. Rev. Lett.* **15**, 524 (1965).
[3] ORTIZ G., HARRIS M., and BALLONE P., *Phys. Rev.* **82**, 5317 (1999).
[4] PARR R. G. and YANG W., *Density-Functional Theory of Atoms and Molecules* (Oxford University Press, New York) 1989.
[5] DREIZLER R. M. and GROSS E. K. U., *Density Functional Theory* (Springer-Verlag, Berlin) 1990.
[6] *A Primer in Density Functional Theory*, Vol. 620 of *Lecture Notes in Physics*, edited by FIOLHAIS C., NOGUEIRA F., and MARQUES M. A. L. (Springer-Verlag, Berlin) 2003.
[7] RUNGE E. and GROSS E. K. U., *Phys. Rev. Lett.* **52**, 997 (1984).
[8] OLIVEIRA L. N., GROSS E. K. U., and KOHN W., *Phys. Rev. Lett.* **60**, 2430 (1988).
[9] KOHN W., GROSS E. K. U., and OLIVEIRA L. N., *J. Phys. (Paris)* **50**, 2601 (1989).
[10] LÜDERS M., Ph.D. thesis, Bayerischen Julius-Maximilians-Universität Würzburg, 1998.
[11] MARQUES M. A. L., Ph.D. thesis, Bayerischen Julius-Maximilians-Universität Würzburg, 2000.
[12] LATHIOTAKIS N. N., MARQUES M. A. L., M. LÜDERS , WIERZBOWSKA M., and GROSS E. K. U., *Int. J. Quantum Chem.* in press (2004).
[13] COLEMAN A. J., *Rev. Mod. Phys.* **35**, 668 (1963).
[14] GILBERT T. L., *Phys. Rev. B* **12**, 2111 (1975).
[15] HOHENBERG P. and KOHN W., *Phys. Rev.* **136**, B864 (1964).
[16] VON BARTH U. and HEDIN L., *J. Phys. C* **5**, 1629 (1972).
[17] KOHN W. and SHAM L. J., *Phys. Rev.* **140**, A1133 (1965).
[18] CEPERLEY D. M. and ALDER B. J., *Phys. Rev. Lett.* **45**, 566 (1980).
[19] PERDEW J. P. and BURKE K., *Int. J. Quantum Chem.* **57**, 309 (1996).
[20] PERDEW J. P., KURTH S., ZUPAN A., and BLAHA P., *Phys. Rev. Lett.* **82**, 2544 (1999), and references therein; ibid, **82**, 5179 (1999) (E).
[21] SHARP R. T. and HORTON G. K., *Phys. Rev.* **90**, 317 (1953).
[22] TALMAN J. D. and SHADWICK W. F., *Phys. Rev. A* **14**, 36 (1976).
[23] PERDEW J. P. and ZUNGER A., *Phys. Rev. B* **23**, 5048 (1981).
[24] MAITRA N. T. and BURKE K., *Phys. Rev. A* **63**, 042501 (2001), ibid **64**, 039901 (2001) (E).
[25] MAITRA N. T., BURKE K., and WOODWARD C., *Phys. Rev. Lett.* **89**, 023002 (2002).
[26] GROSS E. K. U., ULLRICH C. A., and GOSSMAN U. J., in *Density Functional Theory*, Vol. 337 of *NATO ASI, Ser. B*, edited by GROSS E. K. U. and DREIZLER R. (Plenum Press, New York) 1995, .
[27] GROSS E. K. U., DOBSON J. F., and PETERSILKA M., in *Topics in Current Chemistry*, edited by NALEWAJSKI R. F. (Springer Verlag, Heidelberg) 1996, Vol. 181, p. 81.
[28] VAN LEEUWEN R., *Phys. Rev. Lett.* **80**, 1280 (1998).
[29] VAN LEEUWEN R., *Int. J. Mod. Phys. B* **15**, 1969 (2001).
[30] KELDYSH L. V., *Sov. Phys. JETP* **20**, 1018 (1965).
[31] LIU K.-L. and VOSKO S. H., *Can. J. Phys.* **67**, 1015 (1989).
[32] ULLRICH C. A., GOSSMANN U., and GROSS E. K. U., *Phys. Rev. Lett.* **74**, 872 (1995).
[33] KRIEGER J. B., LI Y., and IAFRATE G. J., *Phys. Rev. A* **45**, 101 (1992).
[34] KRIEGER J. B., LI Y., and IAFRATE G. J., in *Density Functional Theory*, Vol. 337 of *NATO ASI, Ser. B*, edited by GROSS E. K. U. and DREIZLER R. (Plenum Press, New York) 1995, .
[35] DOBSON J. F., BÜNNER M. J., and GROSS E. K. U., *Phys. Rev. Lett.* **79**, 1905 (1997).
[36] VIGNALE G., *Phys. Rev. Lett.* **74**, 3233 (1995).

[37] FETTER A. L. and WALECKA J. D., *Quantum Theory of Many-Particle Systems* (McGraw-Hill, New York) 1971.
[38] GROSS E. K. U., RUNGE E., and HEINONEN O., *Many-Particle Theory* (Adam-Hilger, Bristol) 1991.
[39] PETERSILKA M., GOSSMANN U. J., and GROSS E. K. U., *Phys. Rev. Lett.* **76**, 1212 (1996).
[40] CASIDA M., in *Recent developments and applications in density functional theory*, edited by SEMINARIO J. M. (Elsevier, Amsterdam) 1996, p. 391.
[41] BAUERNSCHMITT R. and AHLRICHS R., *Chem. Phys. Lett.* **256**, 454 (1996).
[42] GRABO T., PETERSILKA M., and GROSS E. K. U., *Journal of Molecular Structure (Theochem)* **501**, 353 (2000).
[43] MARCH N. H., RUBIO A., and ALONSO J. A., *J. Phys. B* **32**, 2173 (1999).
[44] PETERSILKA M., GROSS E. K. U., and BURKE K., *Int. J. Quantum Chem.* **80**, 534 (2000).
[45] GONZE X. and SCHEFFLER M., *Phys. Rev. Lett.* **82**, 4416 (1999).
[46] APPEL H., GROSS E. K. U., and BURKE K., *Phys. Rev. Lett.* **90**, 043005 (2003).
[47] GROSS E. K. U. and KOHN W., *Phys. Rev. Lett.* **55**, 2850 (1985).
[48] DOBSON J. F., HARRIS G. H., and O'CONNOR A. J., *J. Phys.: Condens. Matter* **2**, 6461 (1990).
[49] CHAKRAVARTY S., FOGEL M. B., and KOHN W., *Phys. Rev. Lett.* **43**, 775 (1979), ibid **43**, 1451 (1979) (E).
[50] CHAKRAVARTY S., ROSE J. H., WOOD D., and ASHCROFT N. W., *Phys. Rev. B* **24**, 1624 (1981).
[51] DOBSON J. F. and HARRIS G. H., *J. Phys. C: Solid State Phys.* **20**, 6127 (1987).
[52] BURKE K., PETERSILKA M., and GROSS E. K. U., in *Recent Advances in Density Functional Methods*, edited by VARONE V., FANTUCCI P., and BENCINI A. (World Scientific, Singapore) 2002, Vol. III.
[53] TOKATLY I. V. and PANKRATOV O., *Phys. Rev. Lett.* **86**, 2078 (2001).
[54] MARQUES M. A. L., CASTRO A., and RUBIO A., *J. Chem. Phys.* **115**, 3006 (2001).
[55] ZANGWILL A. and SOVEN P., *Phys. Rev. A* **21**, 1561 (1980).
[56] MOORE C. E., *Nat. Stand. Ref. Data Ser.* **35** (United States Government Printing Office, Washington) 1971, Vol. I-III.
[57] YABANA K. and BERTSCH G. F., *Int. J. Quantum Chem.* **75**, 55 (1999).
[58] KOCH E. E. and OTTO A., *Chem. Phys. Lett.* **12**, 476 (1972).
[59] MARQUES M. A. L., CASTRO A., BERTSCH G. F., and RUBIO A., *Computer Phys. Commun.* **151**, 60 (2003).
[60] VASILIEV I., ÖĞÜT S., and CHELIKOWSKY J. R., *Phys. Rev. B* **65**, 115416 (2002).
[61] YABANA K. and BERTSCH G. F., *Phys. Rev. A* **60**, 1271 (1999).
[62] CASTRO A., MARQUES M. A. L., ALONSO J. A., BERTSCH G. F., YABANA K., and RUBIO A., *J. Chem. Phys.* **116**, 1930 (2002).
[63] MARQUES M. A. L., LÓPEZ X., VARSANO D., CASTRO A., and RUBIO A., *Phys. Rev. Lett.* **90**, 258101 (2003).
[64] VAN LEEUWEN R. and BAERENDS E. J., *Phys. Rev. A* **49**, 2421 (1994).
[65] ARYASETIAWAN F., GUNNARSON O., and RUBIO A., *Europhys. Lett.* **57**, 683 (2002).
[66] GRITSENKO O. V., VAN GISBERGEN S. J. A., GÖRLING A., and BAERENDS E. J., *J. Chem. Phys.* **113**, 8478 (2000).
[67] LAUTENSCHLAGER P., GARRIGA M., VIÑA L., and CARDONA M., *Phys. Rev. B* **36**, 4821 (1987).
[68] REINING L., OLEVANO V., RUBIO A., and ONIDA G., *Phys. Rev. Lett.* **88**, 066404 (2002).
[69] ONIDA G., REINIG L., and RUBIO A., *Rev. Mod. Phys.* **74**, 601 (2002).
[70] WAIDMANN S., KNUPFER M., ARNOLD B., FINK J., FLESZAR A., and HANKE W., *Phys. Rev. B* **61**, 10149 (2000).

[71] KIM Y.-H. and GÖRLING A., *Phys. Rev. Lett.* **89**, 096402 (2002).
[72] QIAN Z., CONSTANTINESCU A., and VIGNALE G., *Phys. Rev. Lett.* **90**, 066402 (2003).
[73] MORONI S., CEPERLEY D. M., and SENATORE G., *Phys. Rev. Lett.* **75**, 689 (1995).
[74] IWAMOTO N. and GROSS E. K. U., *Phys. Rev. B* **35**, 3003 (1987).
[75] RICHARDSON C. F. and ASHCROFT N. W., *Phys. Rev. B* **50**, 8170 (1994).
[76] PERDEW J. P. and WANG Y., *Phys. Rev. B* **45**, 13244 (1992).
[77] LEIN M., GROSS E. K. U., and PERDEW J. P., *Phys. Rev. B* **61**, 13431 (2000).
[78] LANGRETH D. C. and PERDEW J. P., *Solid State Commun.* **17**, 1425 (1975).
[79] GUNNARSSON O. and LUNDQVIST B. I., *Phys. Rev. B* **13**, 4274 (1976).
[80] TATARCZYK K., SCHINDLMAYR A., and SCHEFFLER M., *Phys. Rev. B* **63**, 235106 (2001).
[81] BARDEEN J., COOPER L. N., and SCHRIEFFER J. R., *Phys. Rev.* **108**, 1175 (1957).
[82] BARDEEN J. and PINES D., *Phys. Rev.* **99**, 1140 (1955).
[83] MERMIN N. D., *Phys. Rev.* **137**, A1441 (1965).
[84] DE GENNES P. G., *Superconductivity of Metals and Alloys* (Benjamin, New York) 1966.
[85] SUVASINI M. B., TEMMERMAN W. M., and GYORFFY B. L., *Phys. Rev. B* **48**, 1202 (1993).
[86] TEMMERMAN W. M., SZOTEK Z., GYORFFY B. L., ANDERSEN O. K., and JEPSEN O., *Phys. Rev. Lett.* **76**, 307 (1996).
[87] GYORFFY B. L., SZOTEK Z., TEMMERMAN W. M., ANDERSEN O. K., and JEPSEN O., *Phys. Rev. B* **58**, 1025 (1998).
[88] ANDERSEN O. K., JEPSEN O., LIECHTENSTEIN A. I., and MAZIN I. I., *Phys. Rev. B* **49**, 4145 (1994).
[89] ANDERSEN O. K., LIECHTENSTEIN A. I., JEPSEN O., and PAULEN F., *J. Phys. Chem. Solids* **56**, 1573 (1995).
[90] KURTH S., MARQUES M., LÜDERS M., and GROSS E. K. U., *Phys. Rev. Lett.* **83**, 2628 (1999).
[91] GELL-MANN M. and BRUECKNER K. A., *Phys. Rev.* **106**, 364 (1957).
[92] GRAMMATICOS B. and VOROS A., *Ann. Phys. (N.Y.)* **123**, 359 (1979).
[93] ULLRICH C. A. and GROSS E. K. U., *Aust. J. Phys.* **49**, 103 (1995).